

534278

607

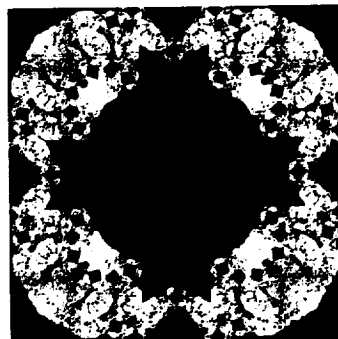
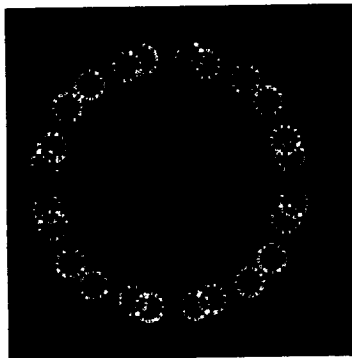
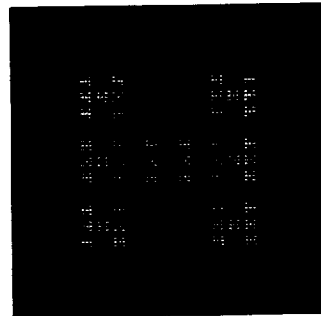
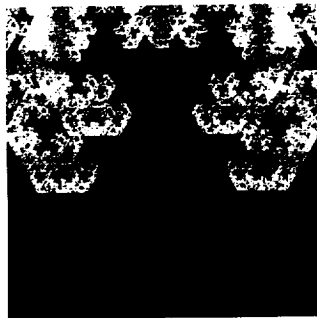
OR

APPLICATIONS

Innovative and Cost-Effective Operations Research Solutions

Fractal Risk Assessment of ISS Propulsion Module in Meteoroid and Orbital Debris Environments

Final Report



Prepared for: NASA-MSFC

By

OR Applications

July 6, 2001

Fractal Risk Assessment of ISS Propulsion Module in Meteoroid and Orbital Debris Environments

TABLE OF CONTENTS

1.0 INTRODUCTION	1
1.1 STUDY OBJECTIVES	2
1.2 EXPECTED SIGNIFICANCE	3
1.3 STATEMENT OF UNIQUENESS	3
1.4 CURRENT SCHEDULE STATUS	3
2.1 TASK 1: INVESTIGATE FRACTAL APPLICABILITY TO METEOROID AND ORBITAL DEBRIS ENVIRONMENTS	4
2.1.1 Sample Meteoroid Environment Fractal Model	4
2.1.2 Orbital Debris Environment Fractal Model	6
2.1.3 Graphical Display of Environment Fractal Models	9
2.2 TASK 2: INVESTIGATE FRACTAL APPLICABILITY TO GEOMETRY MODELING	15
2.2.1 Sample Geometry Fractal Model	15
2.3 TASK 3: INVESTIGATE FRACTAL APPLICABILITY TO HYPERVELOCITY IMPACT PHENOMENOLOGY MODELING	19
2.3.1 Whipple Shield Phenomenology Fractal Model (Orbital Debris)	19
2.3.2 Stuffed Whipple Shield Phenomenology Fractal Model (Orbital Debris)	23
2.3.3 Sample Crater Phenomenology Fractal Model	25
2.3.4 Whipple Shield Phenomenology Fractal Model (Meteoroid Environment)	27
2.3.5 Stuffed Whipple Shield Phenomenology Fractal Model (Meteoroid Environment)	34
2.4 TASK 4: COMPARISON OF FRACTAL RISK ASSESSMENT WITH BUMPER RESULTS	39
2.4.1 Orbital Debris Risk Assessment - Whipple Shield Fractal Model	39
2.4.2 Orbital Debris Risk Assessment - Stuffed Whipple Shield Fractal Model	44
2.4.3 Meteoroid Risk Assessment - Whipple Shield Fractal Model	47
2.4.4 Meteoroid Risk Assessment - Stuffed Whipple Shield Fractal Model	52
2.4.5 Fractal Morphological Studies	54
2.4.6 "Finite Segment" Orbital Debris Risk Assessment - Stuffed Whipple Shield	57
3.0 CONCLUSIONS	59
4.0 RECOMMENDATIONS	61
5.0 REFERENCES	61

Fractal Risk Assessment of ISS Propulsion Module in Meteoroid and Orbital Debris Environments

Abstract

A unique and innovative risk assessment of the International Space Station (ISS) Propulsion Module is conducted using fractal modeling of the Module's response to the meteoroid and orbital debris environments. Both the environment models and structural failure modes due to the resultant hypervelocity impact phenomenology, as well as Module geometry, are investigated for fractal applicability. The fractal risk assessment methodology could produce a greatly simplified alternative to current methodologies, such as BUMPER analyses, while maintaining or increasing the number of complex scenarios that can be assessed. As a minimum, this innovative fractal approach will provide an independent assessment of existing methodologies in a unique way.

1.0 Introduction

The meteoroid and orbital debris environments present considerable challenges to designers of large, long duration spacecraft, such as the ISS Propulsion Module. This Module is a critical part of the ISS, performing altitude and attitude maintenance functions. Since it is a large piece of space hardware with a mission that lasts throughout ISS functionality, the Propulsion Module is expected to sustain and survive thousands of impacts by meteoroid and orbital debris particles. Therefore, a thorough assessment of its ability to withstand these environments is crucial to the success of the ISS mission overall.

Fractals are scale-invariant features that are becoming ubiquitous in the modeling of natural and man-made phenomena. Fractals are represented by simple mathematical models which display surprising degrees of complexity. In many cases, fractals have been found to more fully represent natural and engineering phenomena than much more complex physical and mathematical models. Furthermore, fractals generally require much less data to "fit" the phenomena of interest.

Typically, a meteoroid and orbital debris risk assessment is a complex undertaking. Performing such an assessment generally requires expert information from a number of fields, including space environments, mission analysis, geometry modeling, structural design, and hypervelocity impact phenomenology. Assessments range from inexpensive "back of the envelope" calculations to moderately priced finite element approaches to expensive hydrodynamic analyses. In this field, there is always the question of how complex the assessment should be relative to the presumed and expected accuracy of the results. There is also the issue of error propagation in the assessment. The more complex the assessment, the greater the potential for error at any step of the assessment. Because the environments and structural response are highly nonlinear phenomena, any single error in the analysis can, in general, result in highly inaccurate results.

Because the fractal approach results in greatly simplified model representations, both the costs to assess and the probability of assessment error are greatly reduced. Furthermore,

because simple fractal models result in complex phenomenology, the accuracy of the resulting assessment is not compromised, and could be enhanced. If fractals apply to this field, then a three-way improvement in meteoroid/orbital debris risk assessments could be realized. At the very least, fractals will provide an alternative approach, not previously considered.

The ISS Propulsion Module parameters used in this study are shown in Figure 1.0-1.

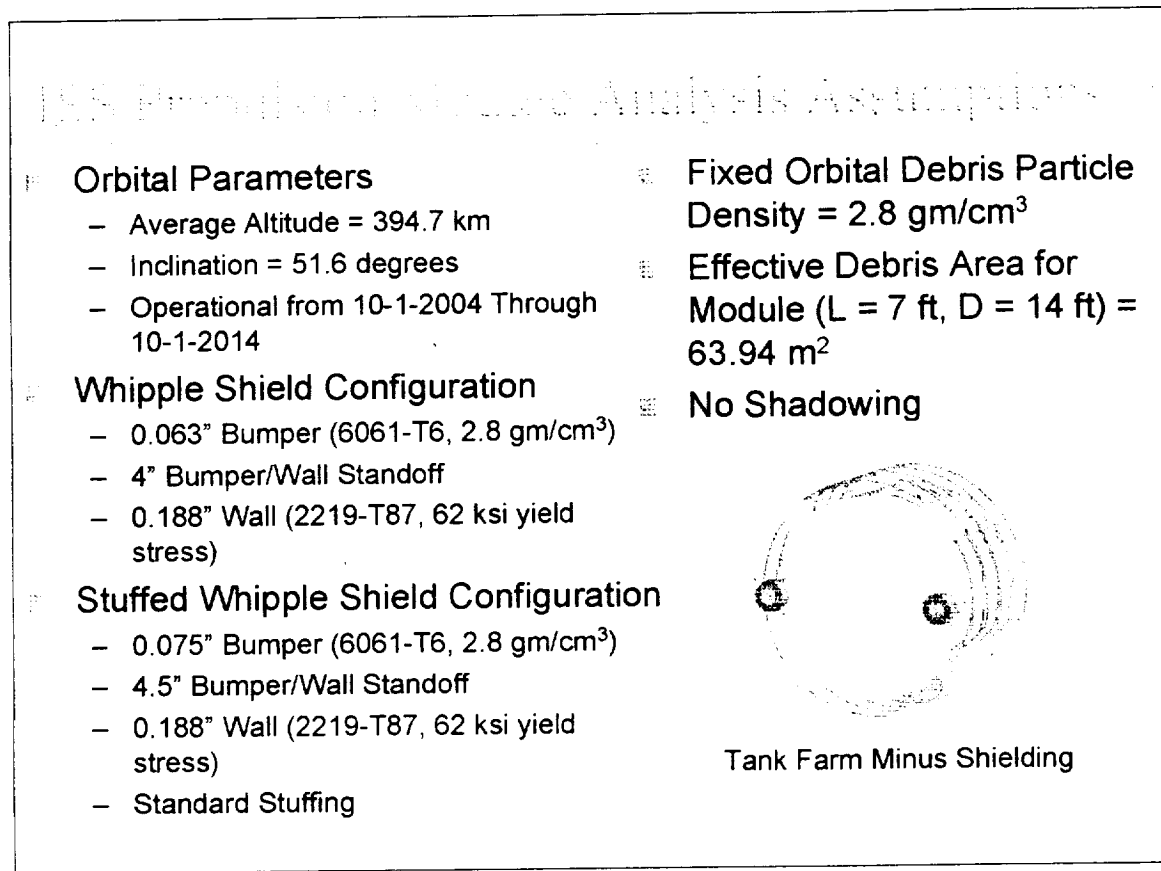


Figure 1.0-1. ISS Propulsion Module Parameters for Meteoroid and Orbital Debris Risk Assessment.

1.1 Study Objectives

The objectives of this study are to investigate the applicability of fractal modeling to meteoroid/orbital debris risk assessment of spacecraft, and, if applicable, to demonstrate such using the ISS Propulsion Module. The study will help answer the following key questions:

1. Can fractal models accurately reflect complex relationships in the meteoroid and orbital debris environments?
 - A. Meteoroid fractal is visually and statistically significant.
 - B. Orbital debris fractal is visually and statistically significant.

2. Can fractal models accurately reflect complexities in geometry modeling of spacecraft?
 - A. Standard shapes are not fractals but are self-similar.
 - B. "Fractal" model has integer dimension.
 - C. Fractal "finite segment" analysis is meaningful at local level and identical in overall risk assessment at global level.
3. Can fractal models accurately reflect complex phenomenology in hypervelocity impact?
 - A. Whipple shield fractal is visually and statistically significant.
 - B. Stuffed Whipple shield fractal is visually and statistically significant.
4. How does a fractal risk assessment of the ISS Propulsion Module compare with an assessment using the traditional spreadsheet analysis?
 - A. Relative error for orbital debris fractal risk assessment is $\pm 0.15\%$ for Whipple Shield and -0.10% for Stuffed Whipple Shield.
 - B. Relative error for meteoroid fractal risk assessment is $\pm 0.025\%$ for Whipple Shield and -0.0014% for Stuffed Whipple Shield.

1.2 Expected Significance

The expected significance of this research and development effort includes an alternative approach to meteoroid/orbital debris risk assessments with the following potential advantages:

1. Reduced analysis complexity.
2. Reduced analysis error,
3. Increased understanding of risk and uncertainty.

1.3 Statement of Uniqueness

The fractal approach has not been previously applied to meteoroid/orbital debris risk assessments of spacecraft.

1.4 Current Schedule Status

All items are completed.

2.1 Task 1: Investigate Fractal Applicability to Meteoroid and Orbital Debris Environments

Under this task, appropriate fractal models for the meteoroid and orbital debris environments are developed. The environments chosen are consistent with those to be experienced by the ISS Propulsion Module. In this task, the environment models, orbital parameters, exposure times, and other applicable mission parameters are baselined relative to the ISS Propulsion Module. Recommendations are provided to MSFC personnel concerning all appropriate models and parameters that maintain consistency between fractal methodologies and BUMPER analyses.

2.1.1 Sample Meteoroid Environment Fractal Model

As an example of the application of fractals to meteoroid/orbital debris environments, consider the portion of the meteoroid environment given by Cour-Palais [1969] as:

$$\begin{aligned} \log_{10}(N) &= -14.37 - 1.213 \log_{10}(m) \\ m &\in [10^{-6}, 1] \end{aligned}$$

where,

N = meteoroid flux (number of particles/m²/sec of mass m or greater),
 m = meteoroid particle mass (gm).

This equation may be rewritten as:

$$N = 10^{-14.37} m^{-1.213}$$

This equation already satisfies the fractal power law property of scale invariance given by:

$$N = cm^{-D}$$

where

c = a constant,

D = the fractal dimension.

Thus, for this portion of the referenced meteoroid environment, the fractal dimension is 1.213. This means that the dimension of the space of interest is between linear and quadratic, tending to be closer to linear. While this fractal may or may not be appropriate

for use in the actual study, it is indicative of the presence of fractals in particulate space environments.

The pertinent meteoroid environment applicable to the ISS Propulsion Module is given by Anderson and Smith [1994]. The flux is given by:

$$F_m(m) = c_0 \{ (c_1 m^{0.306} + c_2)^{-4.38} + c_3 (m + c_4 m^2 + c_5 m^4)^{-0.36} + c_6 (m + c_7 m^2)^{-0.85} \}$$

where

$F_m(m)$ = meteoroid flux (number of particles/m²/year of mass m or greater),

m = meteoroid mass (grams),

$c_0 = 3.156\text{E}07$,

$c_1 = 2.2\text{E}03$,

$c_2 = 15$,

$c_3 = 1.3\text{E}-09$,

$c_4 = 1.0\text{E}11$,

$c_5 = 1.0\text{E}27$,

$c_6 = 1.3\text{E}-16$,

$c_7 = 1.0\text{E}06$.

The density of the meteoroid particle varies with the mass of the particle. Under the assumption of a spherical particle, this density-mass variation corresponds to a density-particle density variation. The "break" points are given in Table 2.1.1-1.

Table 2.1.1-1. Meteoroid Particle Density Break Points

Particle Diameter (cm)	Particle Mass (grams)	Particle Density (gm/cm ³)
$\leq 9.847\text{E}-03$	$\leq 1.0\text{E}-06$	2.0
$> 9.847\text{E}-03$ and < 0.2673	$> 1.0\text{E}-06$ and < 0.01	1.0
≥ 0.2673	≥ 0.01	0.5

Fitting the above model to the simple fractal model, $F_m(m) = cm^{-D}$, we get:

$$F_m(m) = (7.625\text{E} - 08)m^{-1.17824}$$

The percentage variation in this model fit is given by $R = 0.995$, with significance level of $1.79\text{E}-36$, indicating an excellent statistical fit. (Note that all R values reported are for the $\ln(Y) = \ln(a) + b \ln(X)$ model, not for the $Y = a X^b$ model.) Both estimated parameters also showed significance levels corresponding to an excellent fit. Thus, for the referenced meteoroid environment, the fractal dimension is approximately 1.178. This means that the

dimension of the space of interest is between linear and quadratic, tending to be closer to linear.

The fit of this fractal to the actual environment definition is shown below in Figure 2.1.1-1. Notice that the fit is very good, except below particle diameters of $5.0\text{E-}03$ cm, where the fractal tends to overestimate the flux significantly. Particle diameters in this range are not expected to do significant damage to the ISS Propulsion Module, assuming pressure wall perforation is the critical failure mode of concern and that the module shielding is protective in this range of small particles. For the range of particle diameters between $1\text{E-}02$ cm and 0.6 cm, the fractal model underestimates the meteoroid flux relative to the actual model, and above 0.6 cm, the fractal model tends to overestimate the flux relative to the actual model. It is in this final range of particle diameters where the greatest damage potential lies for meteoroid impacts. Therefore, the fractal model would generally be considered to be conservative relative to the actual model.

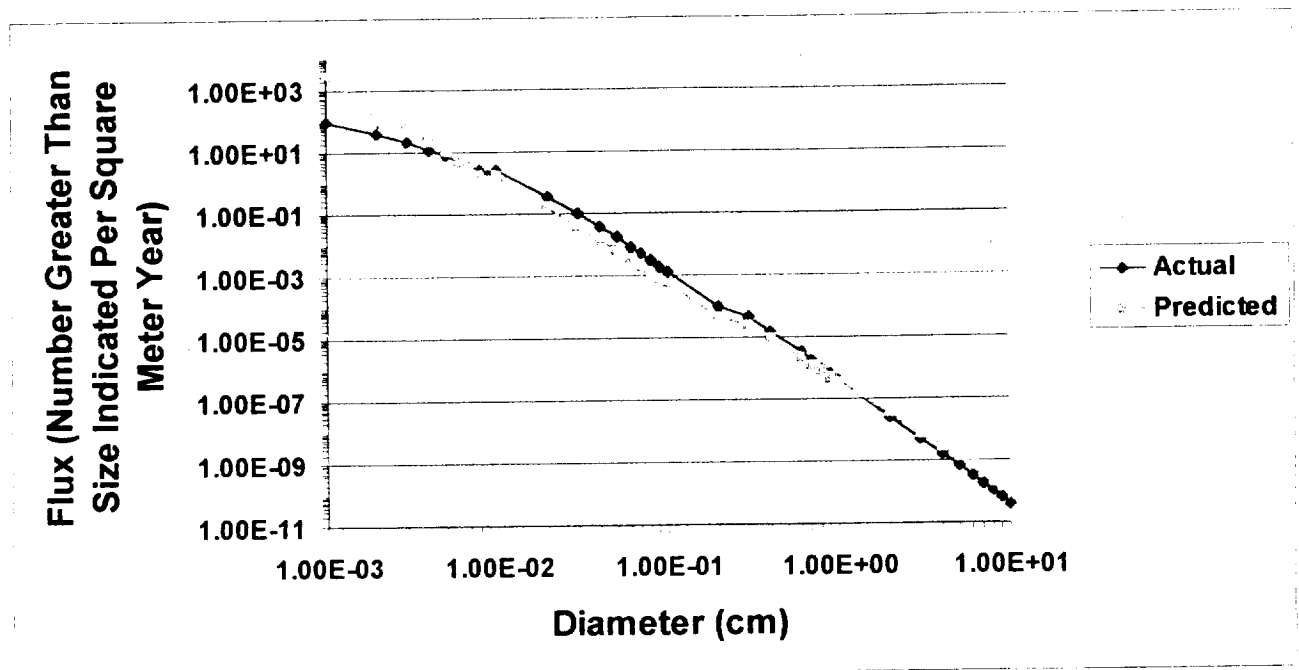


Figure 2.1.1-1. Comparison of Actual vs. Predicted (Fractal) Meteoroid Environment Model

2.1.2 Orbital Debris Environment Fractal Model

The pertinent orbital debris environment applicable to the ISS Propulsion Module is given by Anderson and Smith [1994] in NASA TM-4527. The equations for this model are given by:

$$\begin{aligned}
F_r(d, h, i, t, S) &= H(d) \phi(h, S) \Psi(i) [F_1(d) g_1(t) + F_2(d) g_2(t)] \\
H(d) &= [10^{\exp(-(\log_{10} d - 0.78)^2 / 0.637^2)}]^{1/2} \\
\phi(h, S) &= \phi_1(h, S) / (\phi_1(h, S) + 1) \\
\phi_1(h, S) &= 10^{(h \cdot 200 - S \cdot 140 - 1.5)} \\
F_1(d) &= 1.22 \times 10^{-5} d^{-2.5} \\
F_2(d) &= 8.1 \times 10^{10} (d + 700)^{-6} \\
g_1(t) &= \begin{cases} (1 + q)^{t-1988}, & t < 2011 \\ (1 + q)^{23} (1 + q')^{t-2011}, & t \geq 2011 \end{cases} \\
g_2(t) &= 1 + p(t - 1988)
\end{aligned}$$

where,

F_r = flux, impacts per square meter of surface per year,

d = orbital debris diameter (cm),

t = date (year),

h = altitude (km),

S = 13-month smoothed solar radio flux for $t-1$ year (10^4 Jy),

i = inclination (degrees),

p = annual growth rate of mass in orbit (baseline = 0.05),

q and q' = estimated growth rates of fragment mass (0.02 and 0.04, respectively).

For the ISS Propulsion Module, $h = 394.7$ km, $i = 51.6$ deg, and $t = 10-1-2004$ through 10-1-2014. Figure 2.1.2-1 shows the resulting orbital debris flux for these parameters in the first year of exposure. This figure also shows the corresponding flux from a computer model ORDEM96 for the same mission parameters. It should be noted that the ORDEM96 model appears to use 95%-ile solar flux values, while the flux shown for NASA TM-4527 is derived using 50%-ile solar flux values. Nevertheless, the flux values for the two environment definitions are comparable for particle diameters below about 0.03 cm. Above this threshold, however, the ORDEM96 values are significantly below those for NASA TM-4527.

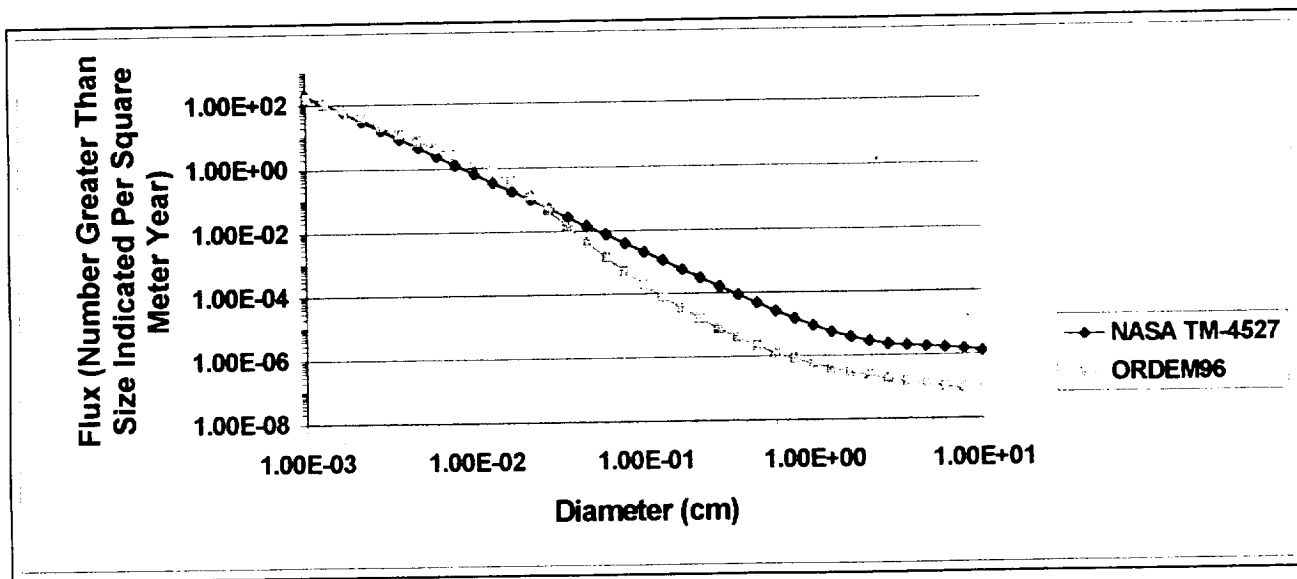


Figure 2.1.2-1. Comparison of NASA TM-4527 vs. ORDEM96 Orbital Debris Environment Models. ISS Propulsion Module Parameters (Orbital debris particles greater than 10 cm are tracked and avoided.)

Using the NASA TM-4527 orbital debris environment definition model, the total mission flux was calculated for the ISS Propulsion Module mission and orbital parameters. This was then fit with a simple fractal model of the form, $F_D(d) = cd^{-D}$, we get:

$$F_D(d) = (2.8435E - 04)d^{-2.1308}$$

The percentage variation in this model fit is given by $R = 0.99$, with significance level of $1.5E-30$, indicating an excellent statistical fit. (Note that all R values reported are for the $\ln(Y) = \ln(a) + b \ln(X)$ model, not for the $Y = a X^b$ model.) Both estimated parameters also showed significance levels corresponding to an excellent fit. Thus, for the referenced orbital debris environment, the fractal dimension is approximately 2.13. This means that the dimension of the space of interest is between quadratic and cubic, tending to be closer to quadratic.

The fit of this fractal to the actual environment definition is shown below. Notice that the fit is very good, except above particle diameters of 4 cm, where the fractal tends to underestimate the flux significantly. Particle diameters in this range may or may not significantly affect the risk calculations for the ISS Propulsion Module. If it is found that this range of particle diameters is a significant consideration, a multifractal (piecewise) approach will be adopted. In that case, the debris environment will be modeled by two or more fractals over various particle diameter ranges. For the range of particle diameters between $1E-03$ cm and $1E-02$ cm, the fractal model underestimates the debris flux relative to the actual model, and from $1E-02$ to 4 cm, the fractal model tends to overestimate the

flux relative to the actual model. It is in this final range of particle diameters where the greatest damage potential lies for orbital debris impacts. Therefore, the fractal model would generally be considered to be conservative relative to the actual model for particle diameters below about 4 cm.

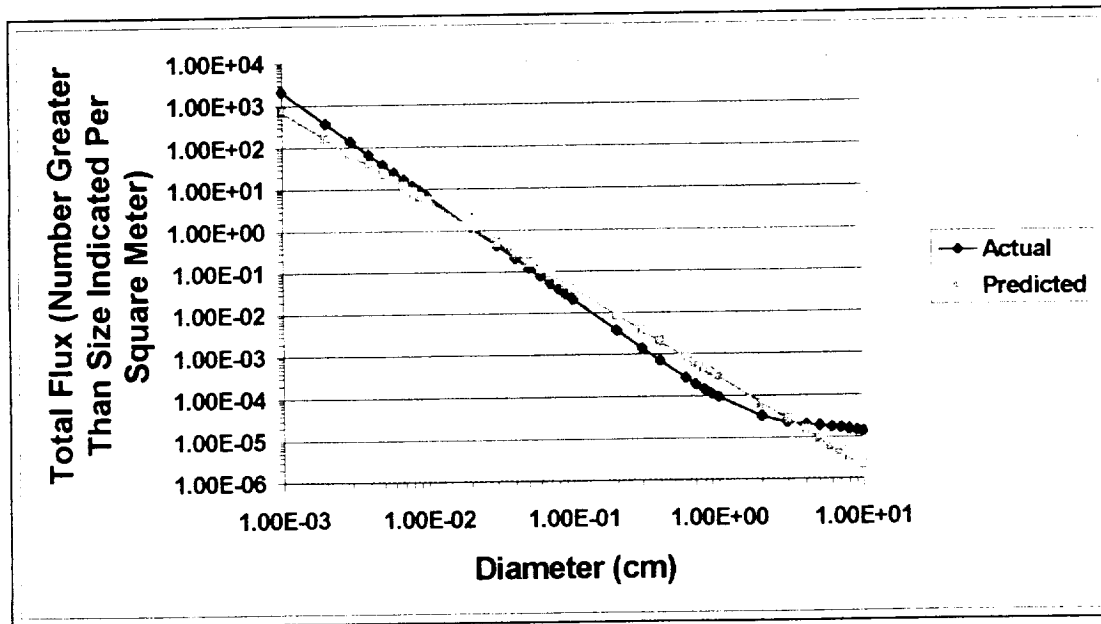
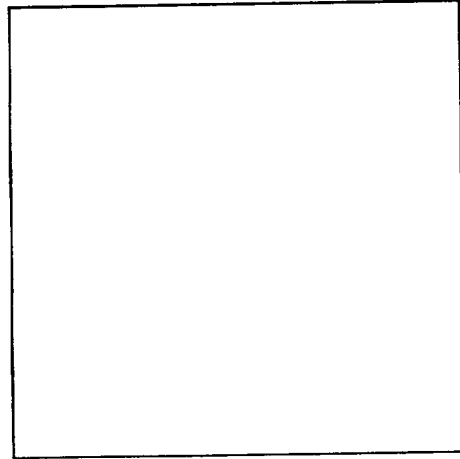


Figure 2.1.2-2. Comparison of Actual vs. Predicted (Fractal) Orbital Debris Environment Models (NASA TM-4527). ISS Propulsion Module Parameters
(Orbital debris particles greater than 10 cm are tracked and avoided.)

2.1.3 Graphical Display of Environment Fractal Models

It was previously published that the orbital debris and meteoroid environment fractal dimensions pertinent to the ISS Propulsion Module are 1.1782 and 2.1308, respectively. How can we graphically display these dimensions in a 2-D way? One way is to consider the unit square:



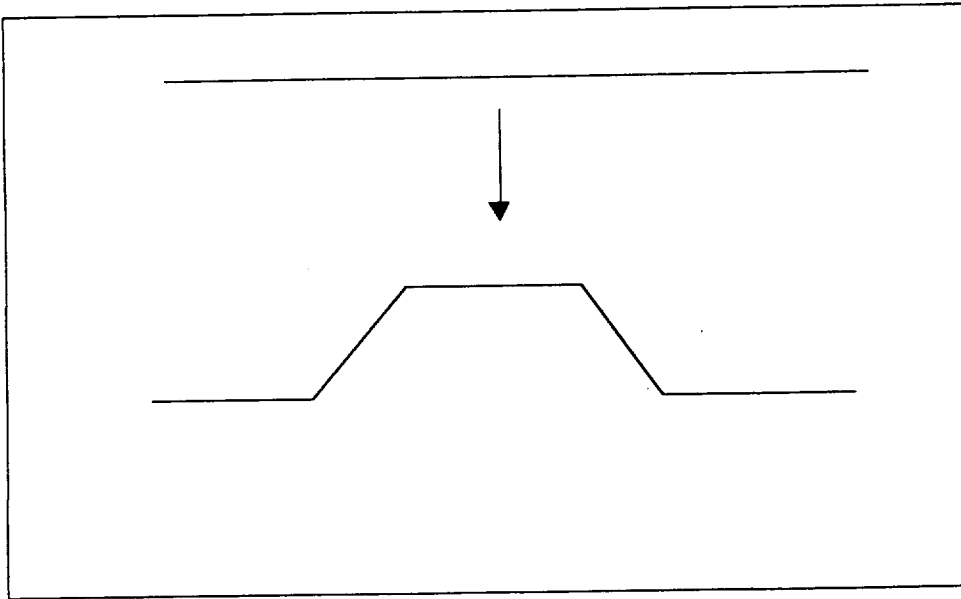
We can replace each line (side) of this square by a series of lines smaller than the original. How do we determine the number of lines and the length of each? One way is to consider the equation:

$$r = N^{\frac{1}{D}}$$

where r = the similarity ratio (the factor by which the line exceeds the reduced lines),
 N = the number of “reduced” lines, and D = the dimension of the fractal.

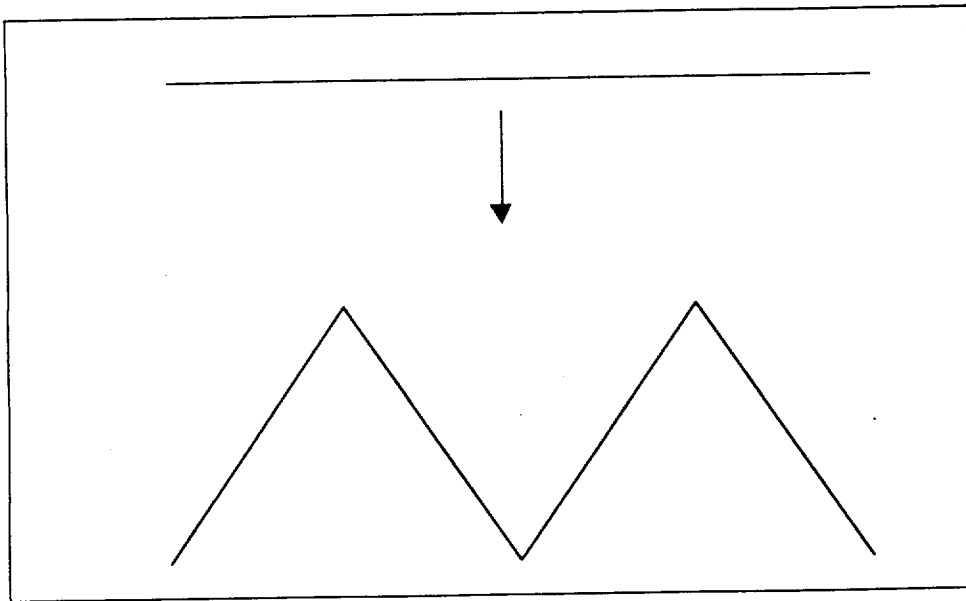
But, how do we determine r and N , given only D ? We desire the smallest values of r and N (to minimize complexity) that satisfy the equation above. Of course, there will always be some error associated with such a requirement for integer values. Hopefully, we can find values that are relatively small, yet produce small errors. In fact, this was achieved for these environments.

For the meteoroid environment ($D = 1.1782$), we find associated values of $r = 4$ and $N = 5$, with an error of only 2% in the determination of r . This means that we can replace each line of the square with 5 lines, each $1/r = 1/4$ the original length. There are a number of ways to achieve this, but we would like to preserve as much symmetry as possible. One method of replacement (formally called a generator) is shown:



Note the symmetry about a vertical line for this replacement scheme. Following the initial replacement, each successive (reduced) line is replaced by 5 lines, each $\frac{1}{4}$ the original length. This process is continued infinitely many times, or until further resolution is impossible. Figure 2.1.3-1 shows the resulting 2-D fractal graphic. This graphic shows four dense regions linked by less dense regions. Notice that the hole in each link represents an identical but much smaller representation of the interior of this graphic. Many other self-similarities are visible in this figure. What technical conclusions, if any, can we draw from such graphical depictions of the meteoroid fractal environment for the ISS Propulsion Module?

For the orbital debris environment ($D = 2.1308$), we find associated values of $r = 2$ and $N = 4$, with an error of only 4% in the determination of r . This means that we can replace each line of the square with 4 lines, each $1/r = 1/2$ the original length. Again, there are a number of ways to achieve this, but we would like to preserve symmetry if possible. A three dimensional representation is preferred for a fractal with dimension greater than 2. However, we can get some graphical feel for this orbital debris fractal in two dimensions. One method of replacement for this fractal is shown:



Again, note the symmetry about a vertical line for this replacement scheme. Following the initial replacement, each successive (reduced) line is replaced by 4 lines, each $1/2$ the original length. This process is continued infinitely many times, or until further resolution is impossible. Figure 2.1.3-2 shows the resulting 2-D fractal graphic for $1/4$ of the total graphic. This graphic shows much higher interior density than that for the meteoroid fractal. This is indicative of the higher dimensionality of the orbital debris environment fractal, relative to that for the meteoroid environment. Notice the cascading identical interiors in the "claw" patterns of this graphic. Many other self-similarities are visible in this figure. What technical conclusions, if any, can we draw from such graphical depictions of the orbital debris fractal environment for the ISS Propulsion Module?

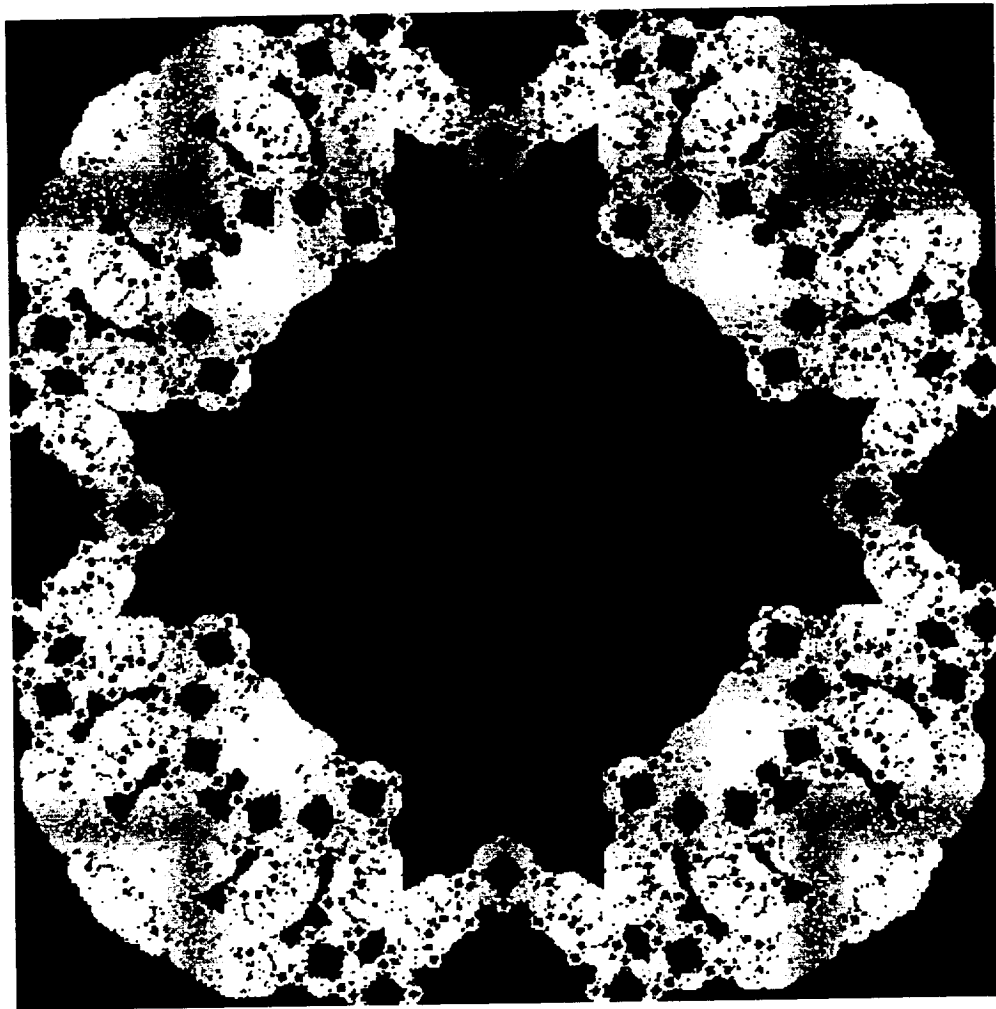


Figure 2.1.3-1. "Smiling Frogs Holding Hands" Fractal Representation of Meteoroid Environment Associated With ISS Propulsion Module (Dimension = 1.1782). Image created by replacing each line of a square by 5 lines, each $\frac{1}{4}$ the length of the original, according to the formula $r = (N)^{1/D}$ where r = scaling factor (4), N = number of lines replacing original line (5), and D = dimension of fractal (1.1782). Error = 2%.
(Image created using BRAZIL DESIGN software.)

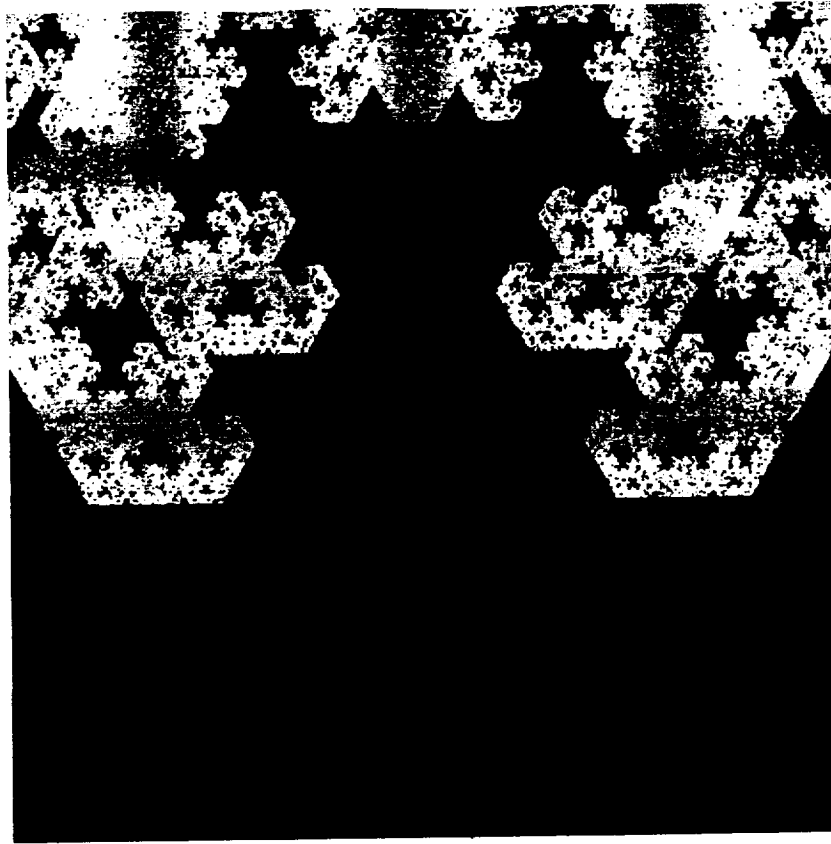


Figure 2.1.3-2. “Debris Claws” One-Fourth of 2-D Fractal Representation of Orbital Debris Environment Associated With ISS Propulsion Module at Altitude of 394.7 km (Dimension = 2.1308). Image created by replacing each line of a square by 4 lines, each 1/2 the length of the original, according to the formula $r = (N)^{1/D}$ where r = scaling factor (2), N = number of lines replacing original line (4), and D = dimension of fractal (2.1308). Error = 4%. Note the higher “interior” density of the orbital debris fractal, as compared to the meteoroid environment fractal. (Image created using BRAZIL DESIGN software.)

2.2 Task 2: Investigate Fractal Applicability to Geometry Modeling

In this task, appropriate fractal models for geometry modeling of spacecraft are developed. The models chosen are consistent with the ISS Propulsion Module. Information on the ISS Propulsion Module geometry, bumper/wall configuration, and BUMPER geometry model is collected and reviewed. Recommendations are provided to MSFC personnel concerning all appropriate models and parameters that maintain consistency between fractal methodologies and BUMPER analyses.

2.2.1 Sample Geometry Fractal Model

As a simple example of the recursive, self-replicating application of fractals to geometry modeling, consider the simple rectangle below. The rectangle is representative of a side view of a cylindrical shaped module, where L is the length of the cylinder and D is the diameter (generally, external) of the cylinder.

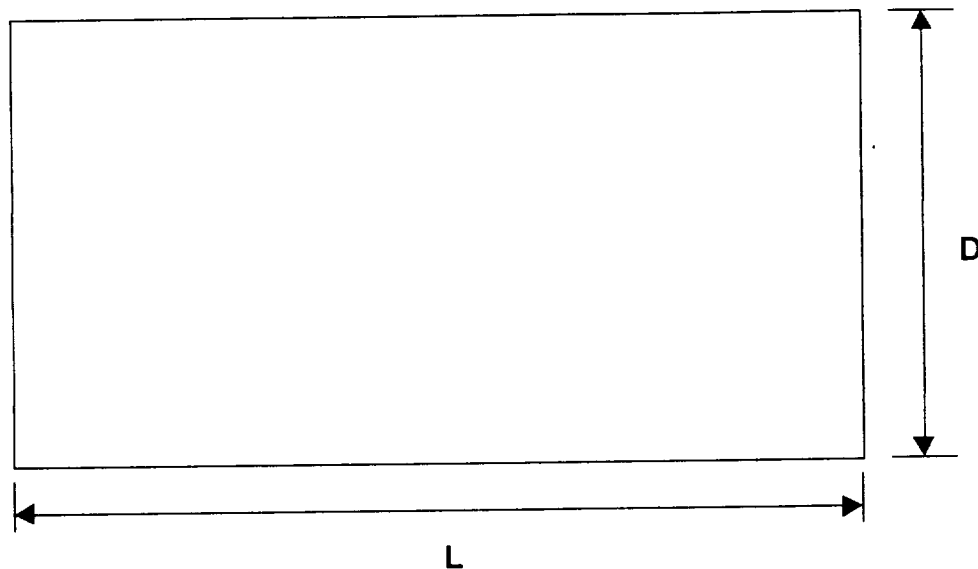


Figure 2.2.1-1. 0th Stage of Fractal Geometry Model

This rectangle might represent, for instance, a highly simplified cross-sectional view of the ISS Propulsion Module. If the recursion rule for this geometry is to halve the rectangle(s) at each step, the second step geometry would look like:

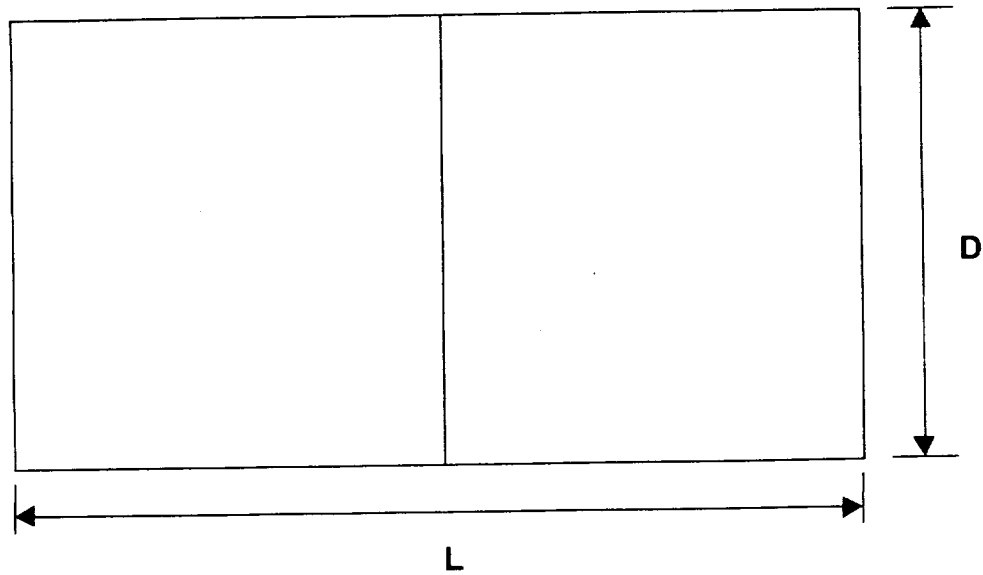


Figure 2.2.1-2. First Stage of Fractal Geometry Model

At the fourth stage, the geometry would appear as follows:

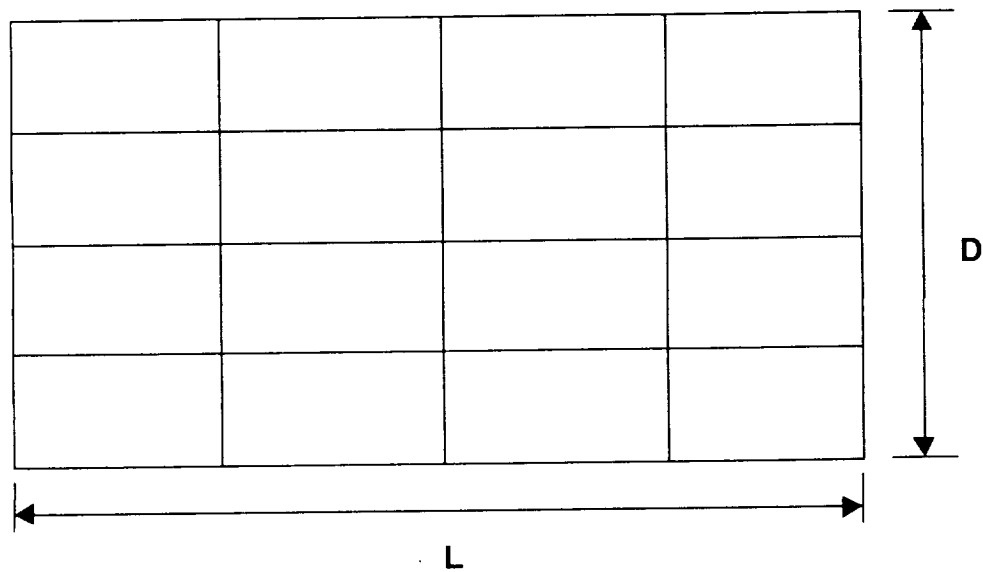


Figure 2.2.1-3. Fourth Stage of Fractal Geometry Model

This stage of the fractal may better represent an idealized version of the cross-section of the ISS Propulsion Module. Other, more complicated examples of geometry modeling can be expected.

Note that the number of subdivided areas (rectangles), $N(A_n)$, is given by:

$$N(A_n) = 2^n, n = 0, 1, 2, 3, \dots$$

where n is the stage of subdivision, and A_n is the area of each individual subarea at this stage. The case, $n = 0$, corresponds to the single original rectangle of area LD . Clearly, there is one such rectangle of area LD , as indicated by the formula. The case, $n = 1$, corresponds to 2 rectangles and the case $n = 4$ corresponds to 16 rectangles, as given by the formula.

Furthermore, the area of each subdivided rectangle at the n th stage, A_n , is given by:

$$A_n = \frac{LD}{2^n}, n = 0, 1, 2, 3, \dots$$

The case $n = 0$ corresponds to the single original rectangle of area LD , $n = 1$ corresponds to two rectangles each of area $LD/2$, and the case $n = 4$ corresponds to 16 rectangles each of area $LD/16$, all correctly predicted by the formula.

Several interesting properties emerge from these simple formula. The first is that:

$$N(A_n) * A_n = (2^n) * \left(\frac{LD}{2^n}\right) = LD, n = 0, 1, 2, 3, \dots$$

Thus, regardless of the number of subdivisions, the product of the number of subareas and the area of each individual subarea is equal to the total original area, LD . This equation may be rewritten as:

$$N(A_n) = LD(A_n)^{-1}, n = 0, 1, 2, 3, \dots$$

This fits the fractal form with $c = LD$, and dimension = 1. Clearly, this is not a fractional exponent, so the term "fractal" is generalized (to include integer values). Nevertheless, the self-similarity of the rectangular subareas is consistent with fractal use.

Also, by the property of a geometric series, the infinite sum of these subareas is given by:

$$\sum_{n=0}^{\infty} A_n = \sum_{n=0}^{\infty} \frac{LD}{2^n} = \frac{LD}{1 - \frac{1}{2}} = 2LD$$

Thus, it follows that the partial sum is given by:

$$\sum_{n=1}^{\infty} A_n = \sum_{n=0}^{\infty} A_n - A_0 = 2LD - \frac{LD}{2^0} = 2LD - LD = LD$$

In this sense, the “fractal” use of self-similar geometric objects may be viewed as either an infinite sum or the product of the number of subareas and the area of each subarea at a given stage of subdivision. Spacecraft shadowing can also be taken into account by limiting the number of areas, $N(A_n)$, at a given stage of subdivision.

A schematic of the ISS Propulsion Module is shown in Figure 2.2.1-4. Projected areas of this configuration can be dealt with in three ways: the standard BUMPER analysis method, or the fractal method, or some combination of both. Each method will be investigated during the geometry, environment, and phenomenology tasks for the meteoroid and/or orbital debris environments.

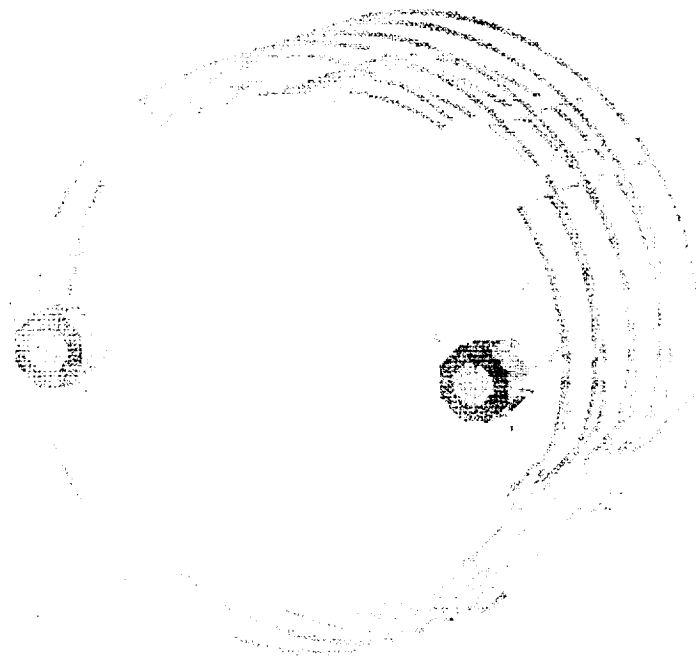


Figure 2.2.1-4. Sketch of ISS Propulsion Module – Tank Farm Minus Shielding
(Courtesy of NASA-MSFC)

2.3 Task 3: Investigate Fractal Applicability to Hypervelocity Impact Phenomenology Modeling

This section involves the development of appropriate fractal models for hypervelocity impact phenomenology modeling of spacecraft. The models chosen are consistent with those applicable to the ISS Propulsion Module. Information on meteoroid/orbital debris critical failure modes, existing penetration equations, and other appropriate quantitative phenomenological models (e.g., crater area, depth) are reviewed and chosen for applicability and comparison to those provided in BUMPER. Recommendations are provided to MSFC personnel concerning all appropriate models and parameters in order to maintain consistency between fractal methodologies, spreadsheet approaches, and BUMPER analyses.

2.3.1 Whipple Shield Phenomenology Fractal Model (Orbital Debris)

A fractal for a Whipple Shield phenomenology model relevant to ISS Propulsion Module is developed in this section.

The Whipple Shield Ballistic Limit model (Christiansen, 1993) is given over three impact velocity ranges as:

$$d_c = [(t_w (\frac{\sigma}{40})^{0.5} + t_b) / (0.6(\cos \theta)^{5/3} \rho_p^{0.5} V^{2/3})]^{18/19}$$

$$V \cos \theta \leq 3 \text{ km / sec}$$

$$d_c = \{[(t_w (\frac{\sigma}{40})^{0.5} + t_b) / (1.248 \rho_p^{0.5} \cos \theta)]^{18/19} (1.75 - (V \cos \theta) / 4)\}$$

$$+ \{[1.071 t_w^{2/3} \rho_p^{-1/3} \rho_b^{-1/9} S^{1/3} (\frac{\sigma}{70})^{1/3}] ((V \cos \theta) / 4 - 0.75)\}$$

$$3 \text{ km / sec} < V \cos \theta < 7 \text{ km / sec}$$

$$d_c = 3.918 t_w^{2/3} \rho_p^{-1/3} \rho_b^{-1/9} (V \cos \theta)^{-2/3} S^{1/3} \left(\frac{\sigma}{70} \right)^{1/3}$$

$$V \cos \theta \geq 7 \text{ km / sec}$$

where:

d_c = critical projectile diameter (cm) causing failure,

ρ = density (g/cm^3),

S = overall spacing between outer bumper and rear wall (cm),

σ = rear wall yield stress (ksi),

t = thickness (cm).

θ = impact angle (deg) measured from surface normal,

V = projectile velocity (km/sec),

with subscripts:

b = bumper,

p = projectile,

w = rear wall.

The configuration analyzed is a Whipple Shield with 0.063" bumper, 4" spacing, and 0.188" rear wall. A ballistic limit curve (critical particle diameter vs. impact velocity) is developed for the orbital debris environment with fixed particle density of 2.8 gm/cm^3 (as specified in the ISS design requirements) using the equations above. A fractal is then fit to this ballistic limit equation. The best fit fractal is given by:

$$d_c = 2.917 V^{-0.6028}$$

This fractal shows an excellent fit to the actual ballistic limit curve. The correlation (R) of 0.991 together with significance level of $4\text{E-}54$ indicates a remarkably good fit by this fractal. (Note that all R values reported are for the $\ln(Y) = \ln(a) + b \ln(X)$ model, not for the $Y = a X^b$ model.) Furthermore, the visual fit shown below in Figure 2.3.1-1 is excellent.

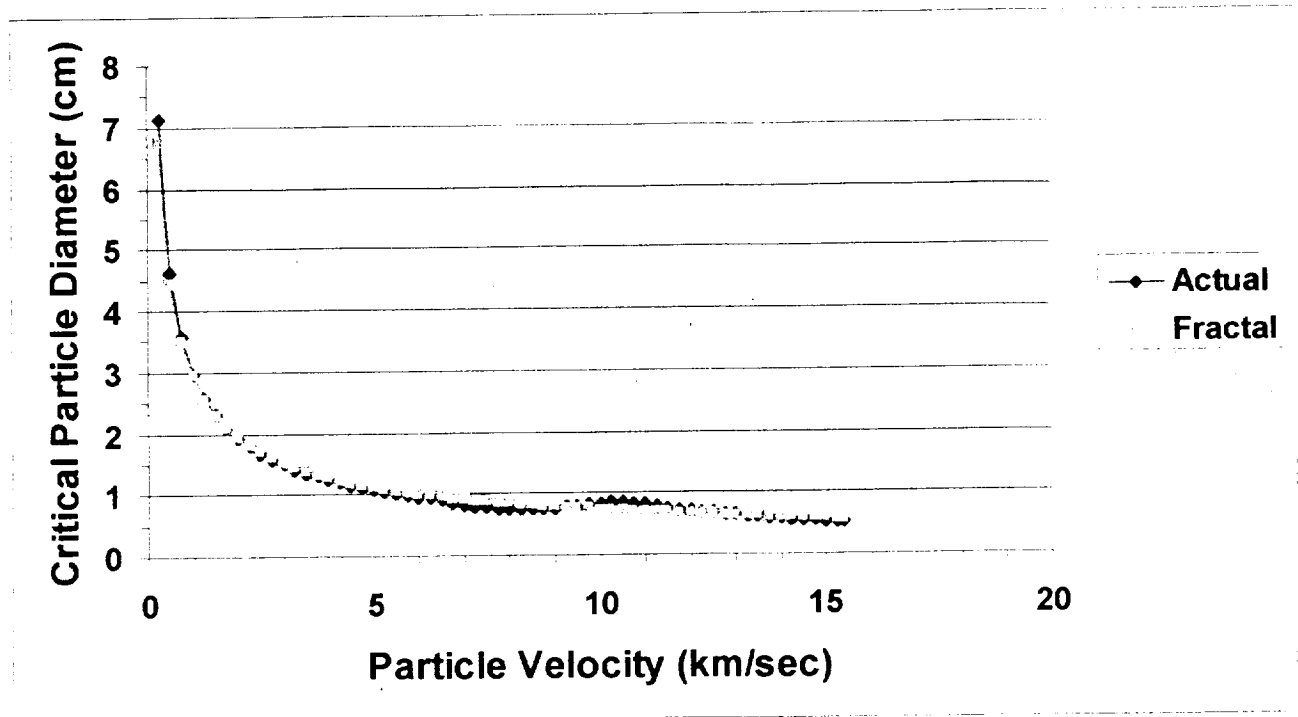


Figure 2.3.1-1. Comparison of actual ballistic limit curve for Whipple shield over orbital debris velocity range with derived fractal model. Both statistical and visual significance indicate an excellent fractal fit. ISS Propulsion Module Parameters

Figure 2.3.1-2 shows the graphical representation for the Whipple Shield phenomenology fractal:

$$D_{crit} = 2.917V^{-0.6028}$$

This graphic was obtained by replacing each line in the unit square by 4 lines, each $1/10^{\text{th}}$ the length of the original line. The relative sparseness of this representation, as compared to the meteoroid and orbital debris flux fractals is indicative of the low fractal dimension, 0.6028.

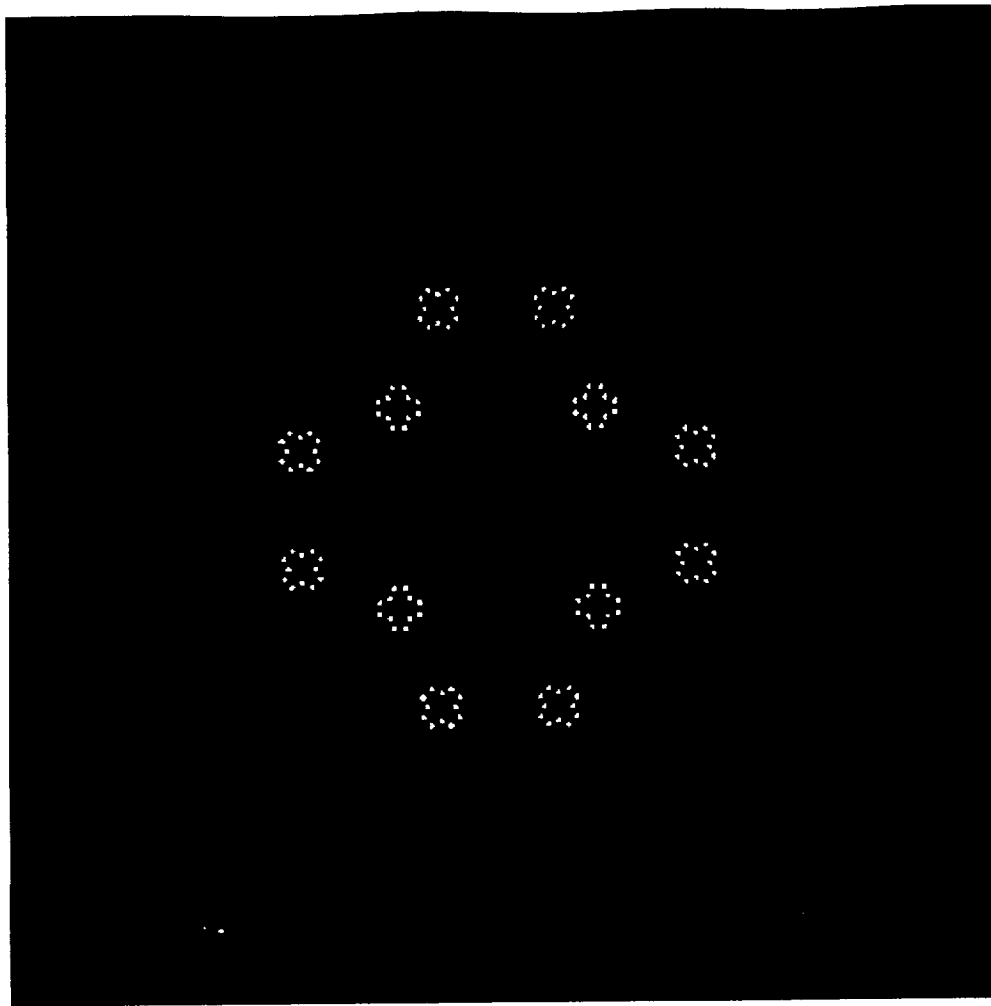


Figure 2.3.1-2. "Impact Pattern" 2-D Fractal Representation of Whipple Shield Phenomenology for Orbital Debris Associated With ISS Propulsion Module at Altitude of 394.7 km (Dimension = 0.6028). Image created by replacing each line of a unit square by 4 lines, each 1/10 the length of the original, according to the formula $r = (N)^{1/D}$ where r = scaling factor (10), N = number of lines replacing original line (4), and D = dimension of fractal (0.6028). Error = 0.3%. Note the lower "interior" density of the phenomenology fractal, as compared to the meteoroid and orbital debris flux fractals.
(Image created using BRAZIL DESIGN software.)

2.3.2 Stuffed Whipple Shield Phenomenology Fractal Model (Orbital Debris)

The equations for the Stuffed Whipple Shield configuration are given in Christiansen et al [1995]. The fractal for the Stuffed Whipple Shield configuration (orbital debris environment) of the ISS Propulsion Module is given by:

$$D_{crit} = 86.73V^{-1.789}$$

Figure 2.3.2-1 shows the visual fit of this fractal (predicted) to the actual data values. The correlation (R) of this fractal model is 0.9766, with a significance level of 9.5E-42, indicating a statistically excellent fit. (Note that all R values reported are for the $\ln(Y) = \ln(a) + b \ln(X)$ model, not for the $Y = aX^b$ model.) The visual fit also appears to be quite good.

Figure 2.3.2-2 shows the graphical representation (1/4 only) for the Stuffed Whipple Shield phenomenology fractal. This graphic was obtained by replacing each line in the unit square by 7 lines, each 1/3 the length of the original line.

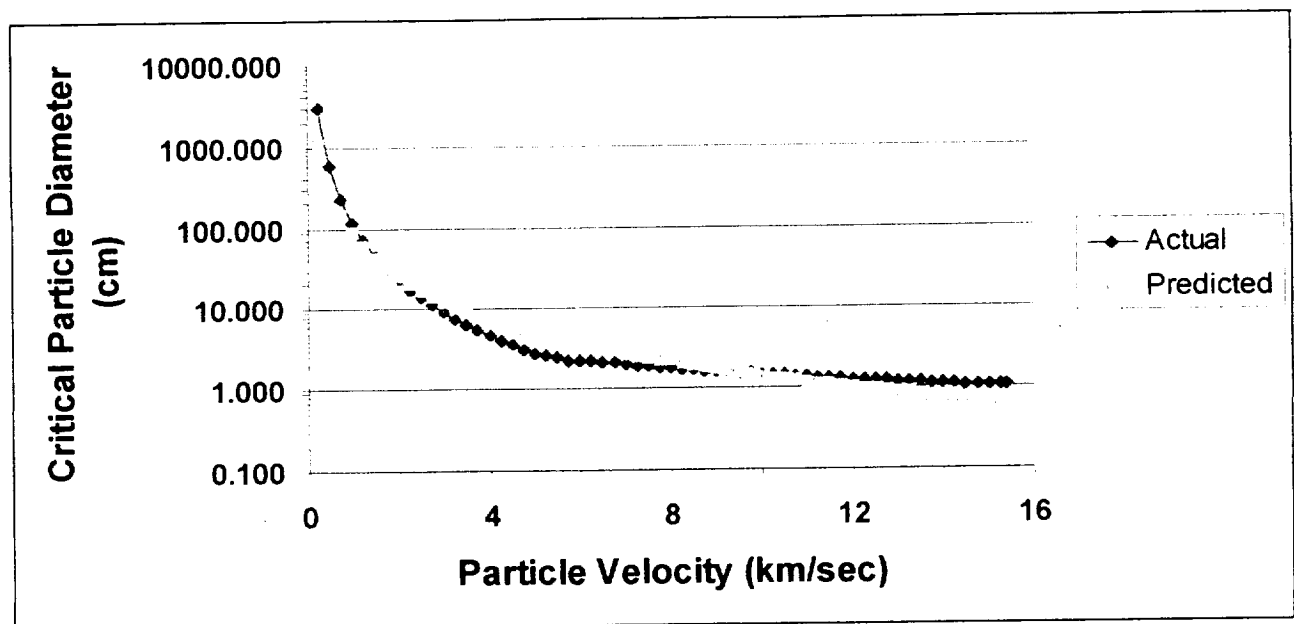


Figure 2.3.2-1. Phenomenology Fractal for Stuffed Whipple Shield Configuration of ISS Propulsion Module. ISS Propulsion Module Parameters

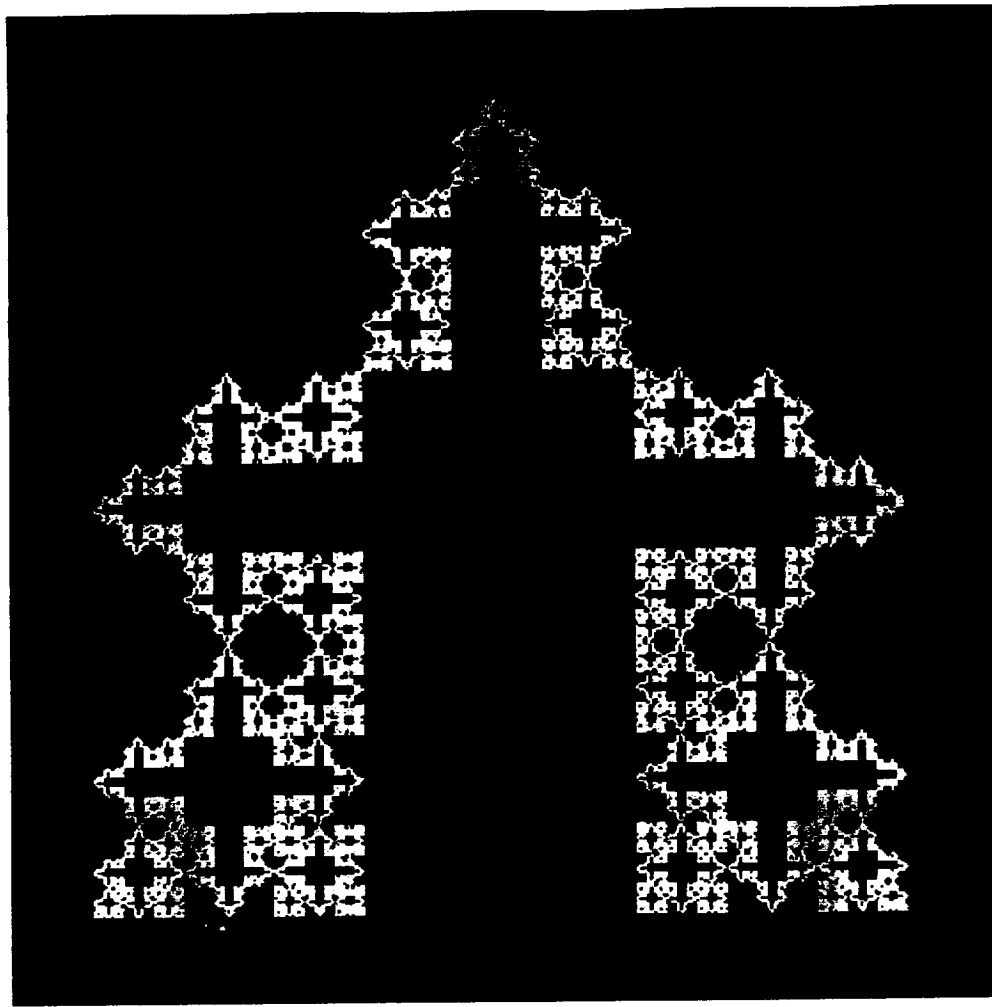


Figure 2.3.2-2. "Cascading Crosses" 2-D Fractal Representation of Stuffed Whipple Shield Phenomenology for Orbital Debris Associated With ISS Propulsion Module at Altitude of 394.7 km (Dimension = 1.789). Image created by replacing each line of a unit square by 7 lines, each 1/3 the length of the original, according to the formula $r = (N)^{1/D}$ where r = scaling factor (3), N = number of lines replacing original line (7), and D = dimension of fractal (1.789). Error = 1%. (Image created using BRAZIL DESIGN software.)

2.3.3 Sample Crater Phenomenology Fractal Model

Klop et al. [1990] present a graph of the fraction of witness plate craters following hypervelocity impact versus the crater diameter. Approximate values from this graph are shown below in Table 2.3.3-1.

Table 2.3.3-1 Approximate Values from Klop et al. [1990] for Experiment 11.

Crater Diameter (mm)	Fraction of Craters With Crater Diameter
0.2	0.15
0.3	0.205
0.4	0.14
0.5	0.1
0.6	0.085
0.7	0.08
0.8	0.06
0.9	0.035
1.0	0.03
1.1	0.025
1.2	0.022
1.3	0.015
1.4	0.01
1.5	0.004
1.6	0.02
1.7	0.004
1.8	0.0001
1.9	0.004
2.0	0.0001
2.1	0.004
2.2	0.0018

The power law for fractals in this case is given by:

$$f_c = a d_c^{-D}$$

where

f_c = the fraction of craters with diameter at least as great as d_c ,

a = a constant,

d_c = the crater diameter (mm),

D = the fractal dimension.

Regression of Table 2.3.3-1 values results in the following fractal equation:

$$f_c = 0.0713d_c^{-2.505}$$

$$d_c \in [0.35, 2.25]$$

The correlation for this regression is $R = 0.922$, while the significance level is $\alpha = 3.03\text{E-}09$, indicating a highly significant model from a statistical standpoint. (Note that all R values reported are for the $\ln(Y) = \ln(a) + b \ln(X)$ model, not for the $Y = a X^b$ model.) Using this model, we see that the fractal dimension for crater diameter features on the witness plate is approximately 2.5. This means that the dimension of the space of crater diameters is roughly halfway between quadratic (2-D) and cubic (3-D). Note, too, that if the equation above is changed to model the total number of craters instead of the fraction of craters, the coefficient will change, but the exponent will not. Thus, the fractal dimension will remain the same regardless of the method of data normalization. Figure 2.3.3-1 shows this relationship. The area of the bubbles, while not to scale, represent the relative projected areas of the craters for a given crater diameter. While this fractal may or may not be appropriate for use, it is indicative of the presence of fractals in hypervelocity impact phenomenology models other than those for ballistic limit curves.

Figure 2.3.3-2 shows the corresponding graphical representation for $\frac{1}{4}$ of this fractal. Note the relatively higher fractal density of this graphic. This is due to the high dimension (2.505) associated with this fractal.

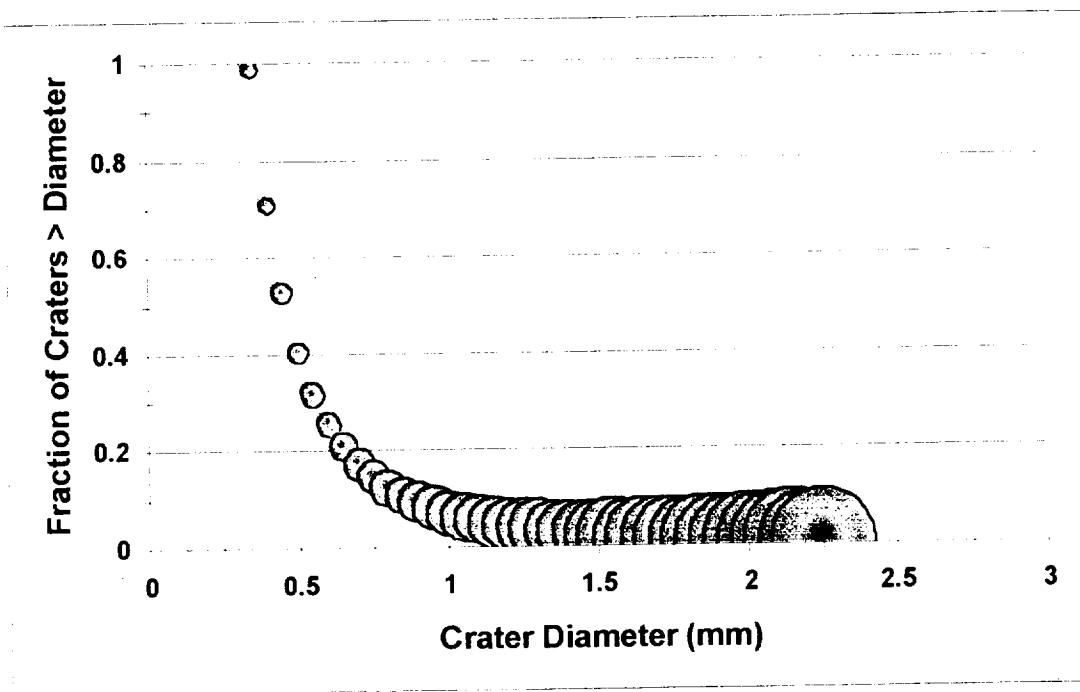


Figure 2.3.3-1. Fraction of Craters Greater Than Given Crater Diameters

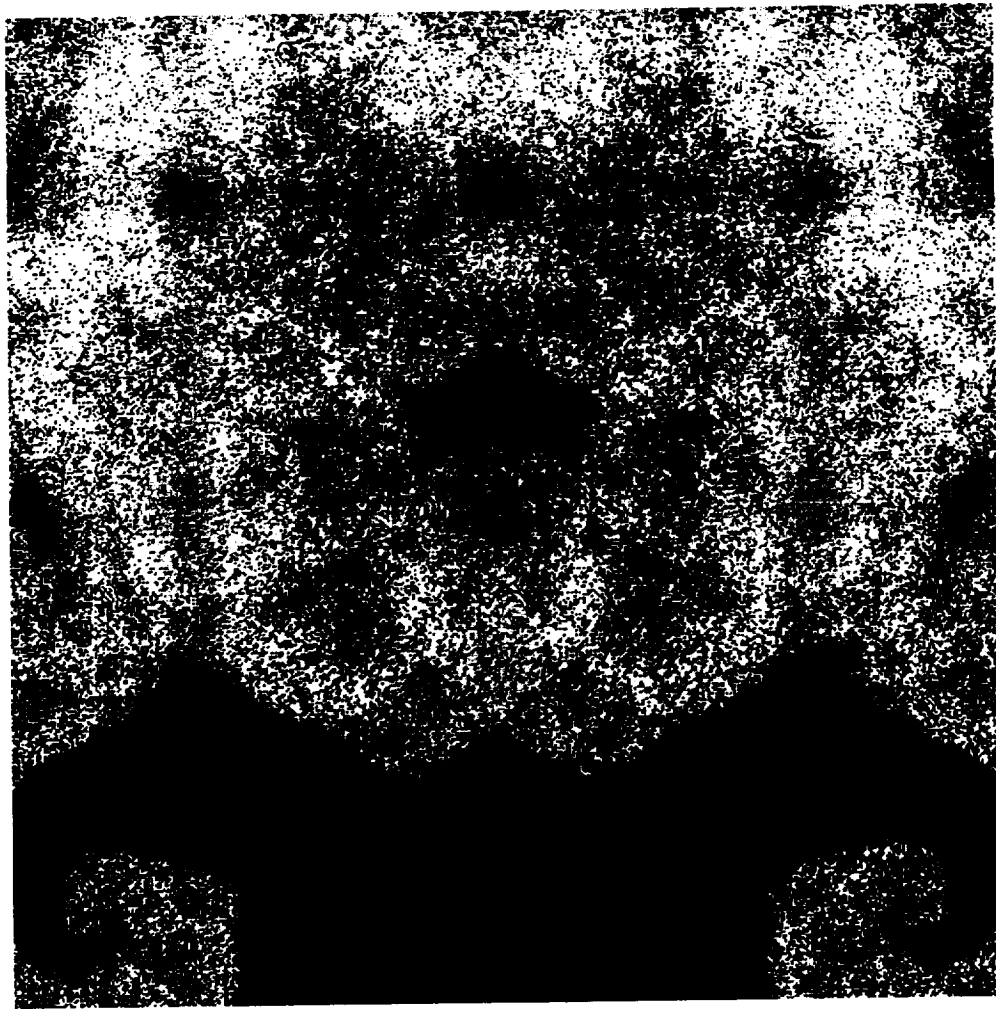


Figure 2.3.3-2. "Upside Down Smiling Frog Flexing Biceps" 2-D Fractal Representation of Crater Phenomenology (Dimension = 2.505). Image created by replacing each line of a unit square by 6 lines, each 1/2 the length of the original, according to the formula $r = (N)^{1/D}$ where r = scaling factor (2), N = number of lines replacing original line (6), and D = dimension of fractal (2.505). Error = 2%. Greater fractal density represents higher fractal dimensionality. (Image created using BRAZIL DESIGN software.)

2.3.4 Whipple Shield Phenomenology Fractal Model (Meteoroid Environment)

A fractal for a Whipple Shield phenomenology model relevant to ISS Propulsion Module in the meteoroid environment is developed in this section.

The Whipple Shield Ballistic Limit model (Christiansen, 1993) is given over three impact velocity ranges as:

$$d_c = [(t_w (\frac{\sigma}{40})^{0.5} + t_b) / (0.6(\cos \theta)^{5/3} \rho_p^{0.5} V^{2/3})]^{18/19}$$

$$V \cos \theta \leq 3 \text{ km / sec}$$

$$d_c = \{[(t_w (\frac{\sigma}{40})^{0.5} + t_b) / (1.248 \rho_p^{0.5} \cos \theta)]^{18/19} (1.75 - (V \cos \theta) / 4)\}$$

$$+ \{[1.071 t_w^{2/3} \rho_p^{-1/3} \rho_b^{-1/9} S^{1/3} (\frac{\sigma}{70})^{1/3}] ((V \cos \theta) / 4 - 0.75)\}$$

$$3 \text{ km / sec} < V \cos \theta < 7 \text{ km / sec}$$

$$d_c = 3.918 t_w^{2/3} \rho_p^{-1/3} \rho_b^{-1/9} (V \cos \theta)^{-2/3} S^{1/3} (\frac{\sigma}{70})^{1/3}$$

$$V \cos \theta \geq 7 \text{ km / sec}$$

where:

d_c = critical projectile diameter (cm) causing failure,

ρ = density (g/cm^3),

S = overall spacing between outer bumper and rear wall (cm),

σ = rear wall yield stress (ksi),

t = thickness (cm).

θ = impact angle (deg) measured from surface normal,

V = projectile velocity (km/sec),

with subscripts:

b = bumper,

p = projectile,

w = rear wall.

The configuration analyzed is a Whipple Shield with 0.063" bumper, 4" spacing, and 0.188" rear wall. A ballistic limit curve (critical particle diameter vs. impact velocity) is developed for the meteoroid environment using the equations above. A fractal is then fit to this ballistic limit equation. The best fit fractal is given by:

$$d_c = 7.016 V^{-0.8143} (\theta + 1)^{0.1595}$$

This fractal shows an excellent fit to the actual ballistic limit curve. The correlation (R) of 0.886 together with significance level of 3E-144 indicates a remarkably good fit by this fractal. (Note that all R values reported are for the $\ln(Y) = \ln(a) + b \ln(X)$ model, not for the $Y = a X^b$ model.) The visual fits for various values of impact angle are shown below in Figures 2.3.4-1 through 2.3.4-7.

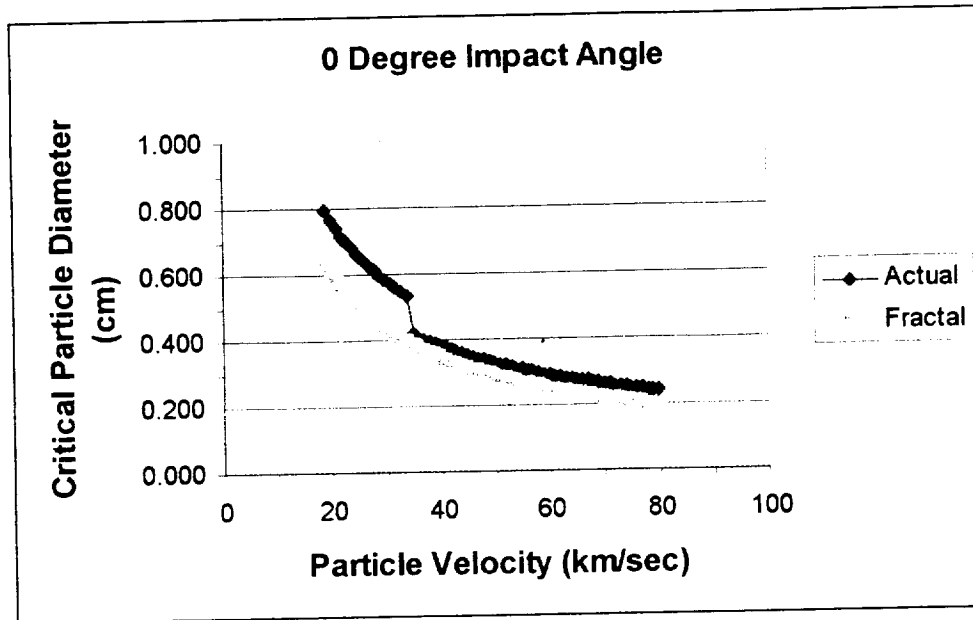


Figure 2.3.4-1. Comparison of actual ballistic limit curve for Whipple shield over meteoroid velocity range (0 degree impact angle) with derived fractal model.
ISS Propulsion Module Parameters

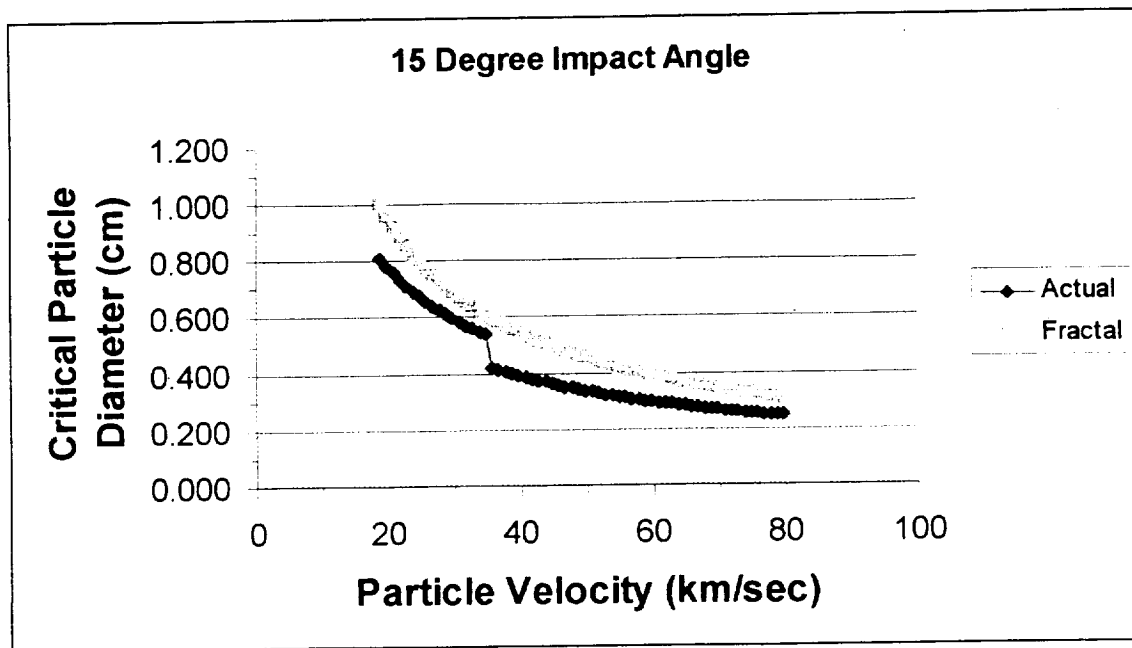


Figure 2.3.4-2. Comparison of actual ballistic limit curve for Whipple shield over meteoroid velocity range (15 degree impact angle) with derived fractal model.
ISS Propulsion Module Parameters

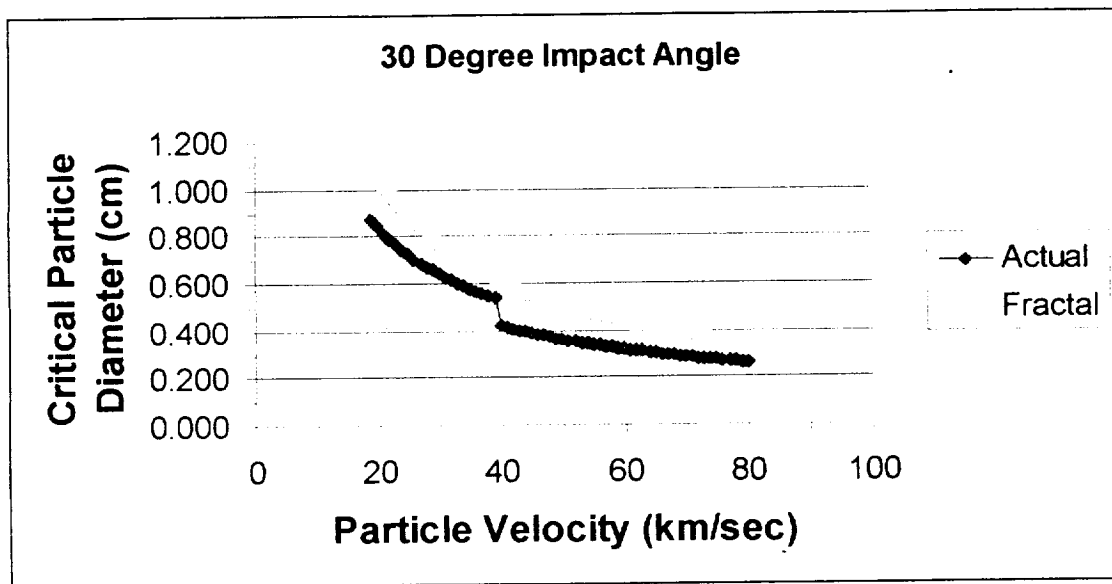


Figure 2.3.4-3. Comparison of actual ballistic limit curve for Whipple shield over meteoroid velocity range (30 degree impact angle) with derived fractal model.
ISS Propulsion Module Parameters

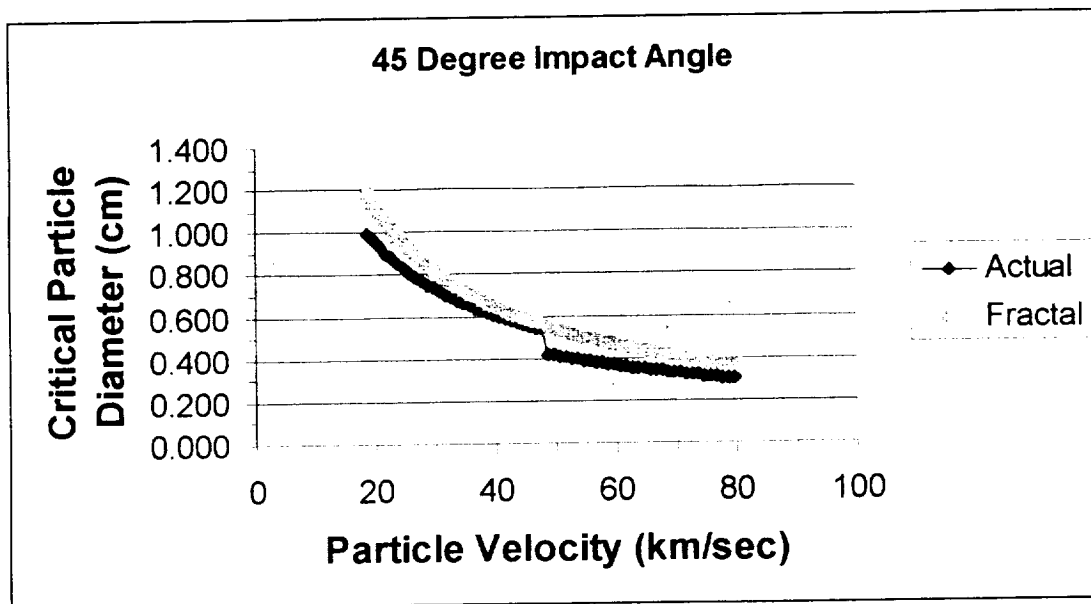


Figure 2.3.4-4. Comparison of actual ballistic limit curve for Whipple shield over meteoroid velocity range (45 degree impact angle) with derived fractal model. ISS Propulsion Module Parameters

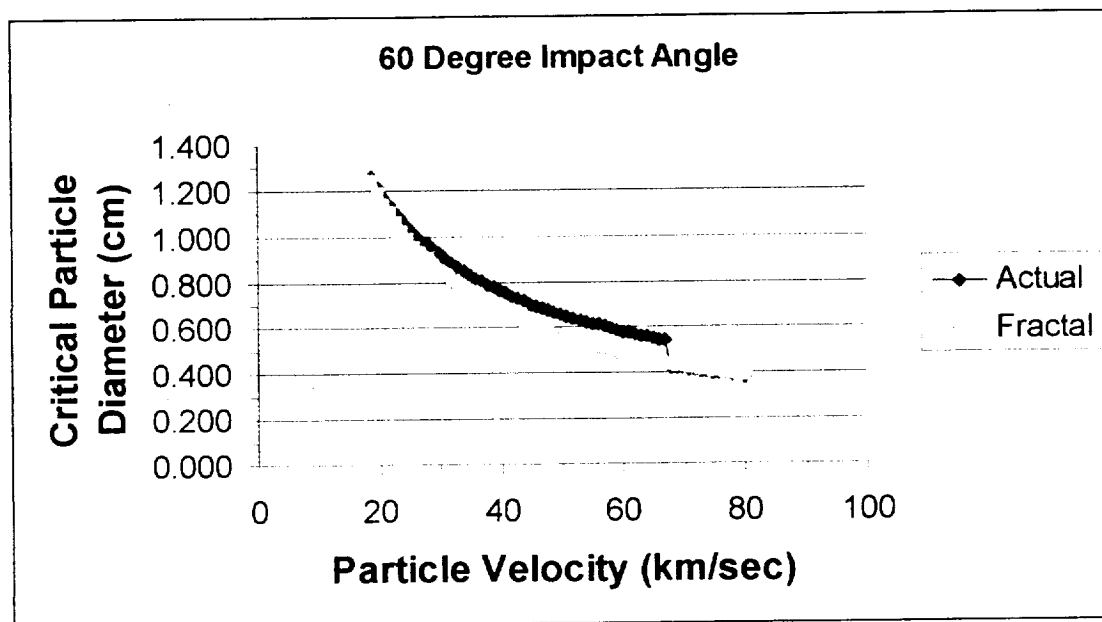


Figure 2.3.4-5. Comparison of actual ballistic limit curve for Whipple shield over meteoroid velocity range (60 degree impact angle) with derived fractal model. ISS Propulsion Module Parameters

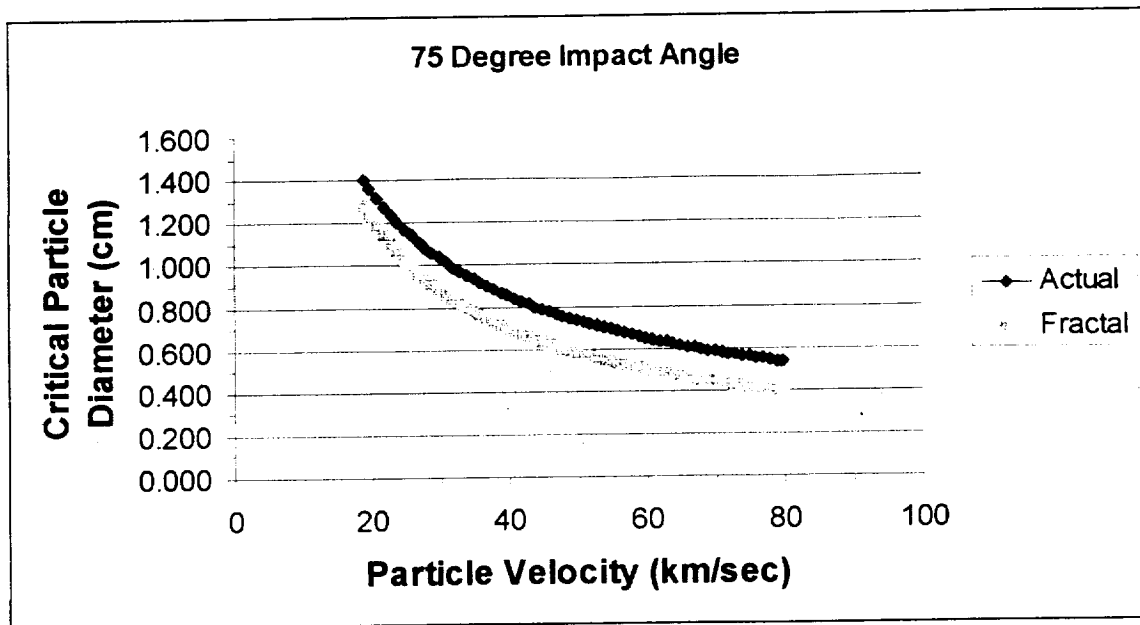


Figure 2.3.4-6. Comparison of actual ballistic limit curve for Whipple shield over meteoroid velocity range (75 degree impact angle) with derived fractal model. ISS Propulsion Module Parameters

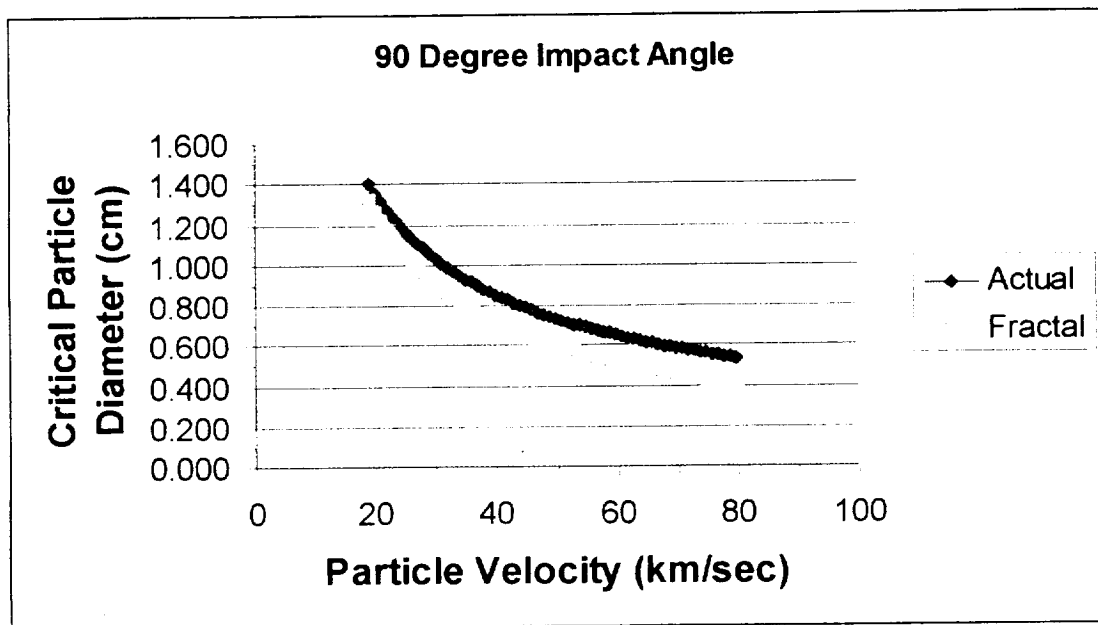


Figure 2.3.4-7. Comparison of actual ballistic limit curve for Whipple shield over meteoroid velocity range (90 degree impact angle) with derived fractal model. ISS Propulsion Module Parameters

Figure 2.3.4-8 shows the graphical representation for the Whipple Shield phenomenology fractal:

$$D_{crit} = 7.016V^{-0.8143}(\theta + 1)^{0.1595}$$

This graphic was obtained by replacing each line in the unit square by 6 lines, each 1/9th the length of the original line. The fractal variable shown is velocity, with fractal dimension of 0.8143.

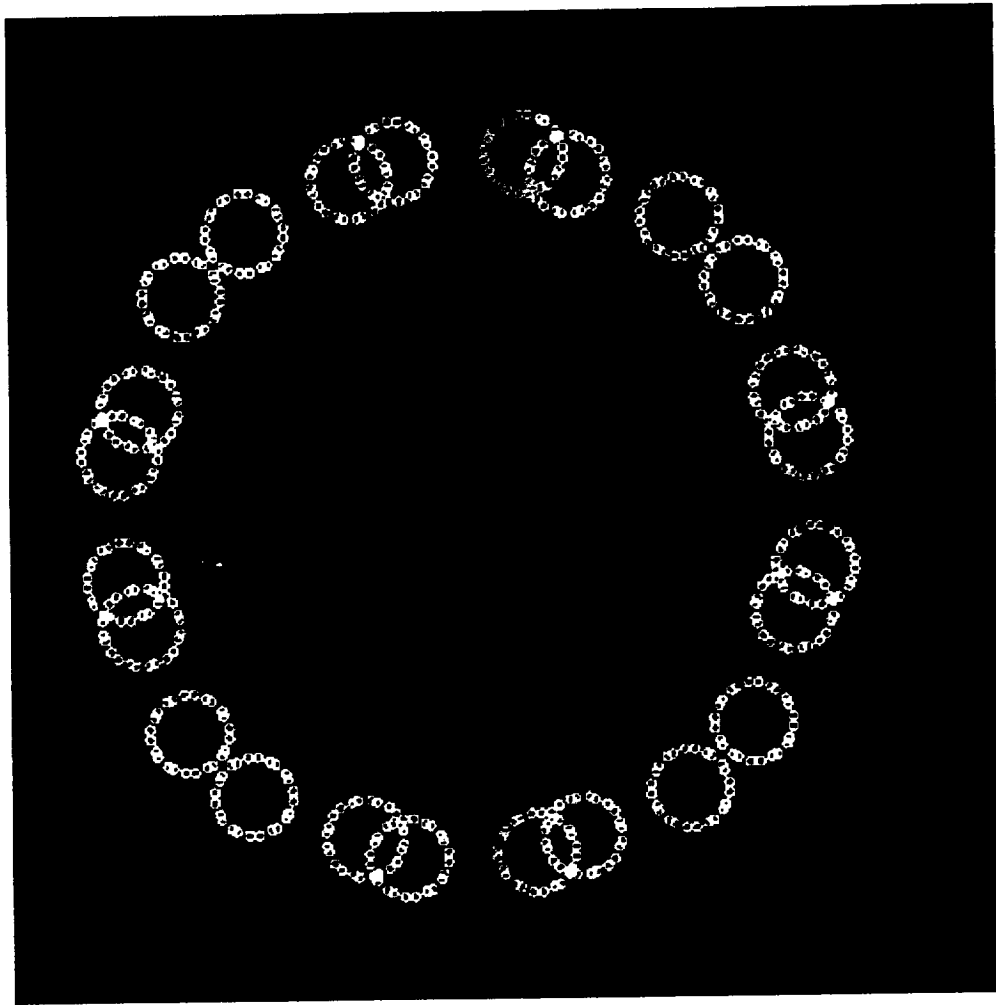


Figure 2.3.4-8. "Circle of Circles" 2-D Fractal Representation of Whipple Shield Phenomenology for Meteoroids Associated With ISS Propulsion Module at Altitude of 394.7 km (Dimension = 0.8143). Image created by replacing each line of a unit square by 6 lines, each 1/9 the length of the original, according to the formula $r = (N)^{1/D}$ where r = scaling factor (9), N = number of lines replacing original line (6), and D = dimension of fractal (0.8143). Error = 0.33%. (Image created using BRAZIL DESIGN software.)

2.3.5 Stuffed Whipple Shield Phenomenology Fractal Model (Meteoroid Environment)

The equations for the Stuffed Whipple Shield configuration are given in Christiansen et al [1995]. The fractal for the Stuffed Whipple Shield configuration (meteoroid environment) of the ISS Propulsion Module is given by:

$$D_{crit} = 6.81V^{-0.5319}(\theta + 1)^{0.2679}$$

Figures 2.3.5-1 through 2.3.5-7 show the visual fits of this fractal to the actual data values for various particle impact angles. The correlation (R) of this fractal model is 0.515, with a significance level of 1.4E-29, indicating a statistically excellent fit. (Note that all R values reported are for the $\ln(Y) = \ln(a) + b \ln(X)$ model, not for the $Y = a X^b$ model.) The main reason for the relatively low R value is the exceedingly high critical particle diameters for low velocities and impact angle of 89 degrees.

Figure 2.3.5-8 shows the graphical representation for the Stuffed Whipple Shield phenomenology fractal. This graphic was obtained by replacing each line in the unit square by 3 lines, each 1/8 the length of the original line.

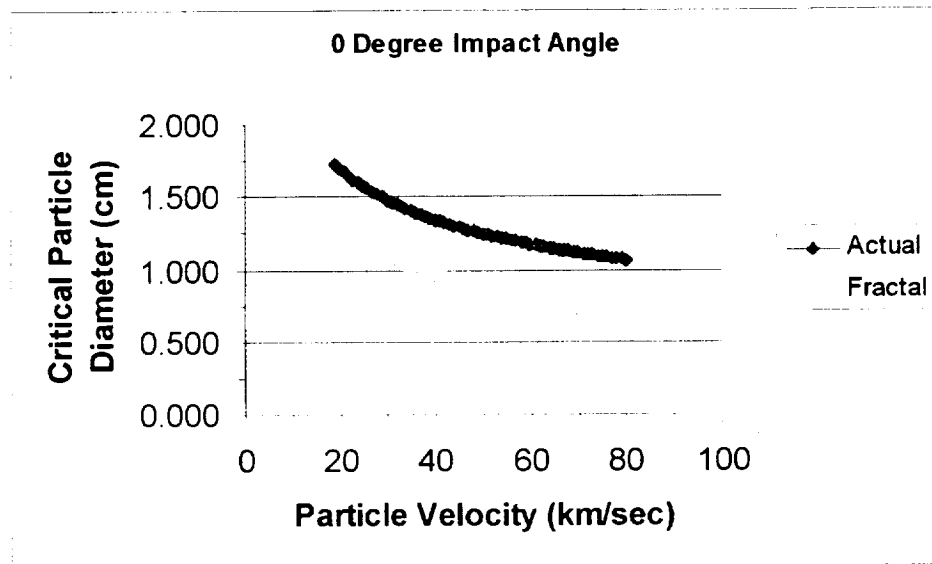
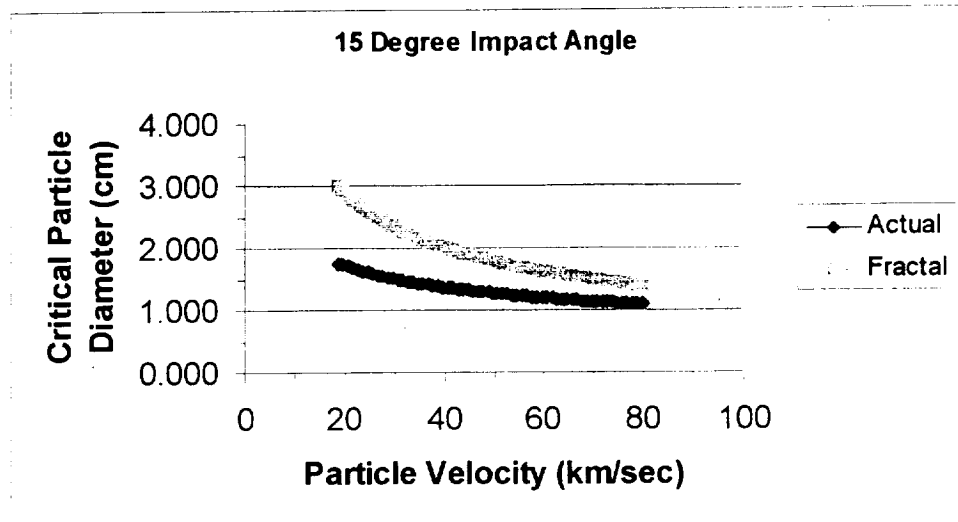
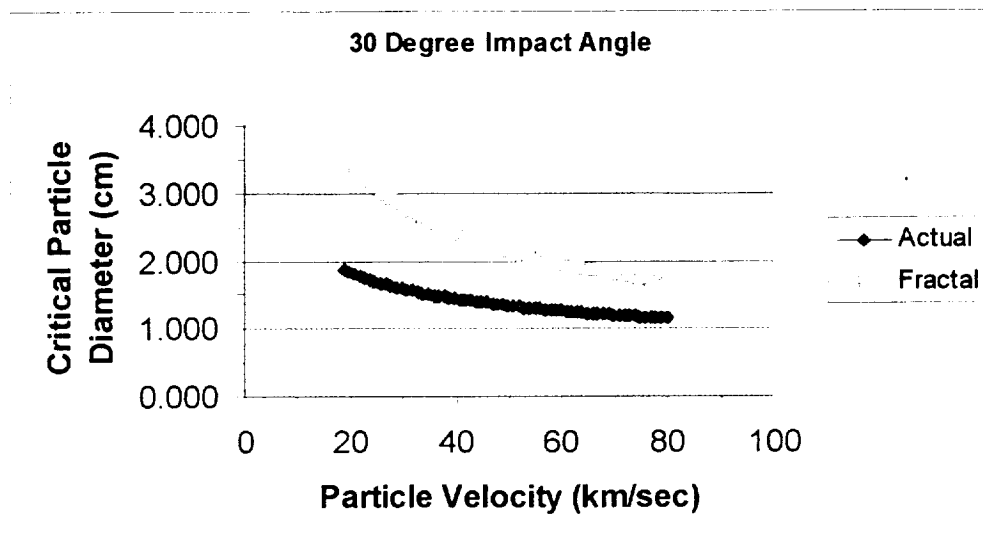


Figure 2.3.5-1. Phenomenology Fractal for Stuffed Whipple Shield Configuration of ISS Propulsion Module in Meteoroid Environment (0 degree impact angle).
ISS Propulsion Module Parameters



**Figure 2.3.5-2. Phenomenology Fractal for Stuffed Whipple Shield Configuration of ISS Propulsion Module in Meteoroid Environment (15 degree impact angle).
ISS Propulsion Module Parameters**



**Figure 2.3.5-3. Phenomenology Fractal for Stuffed Whipple Shield Configuration of ISS Propulsion Module in Meteoroid Environment (30 degree impact angle).
ISS Propulsion Module Parameters**

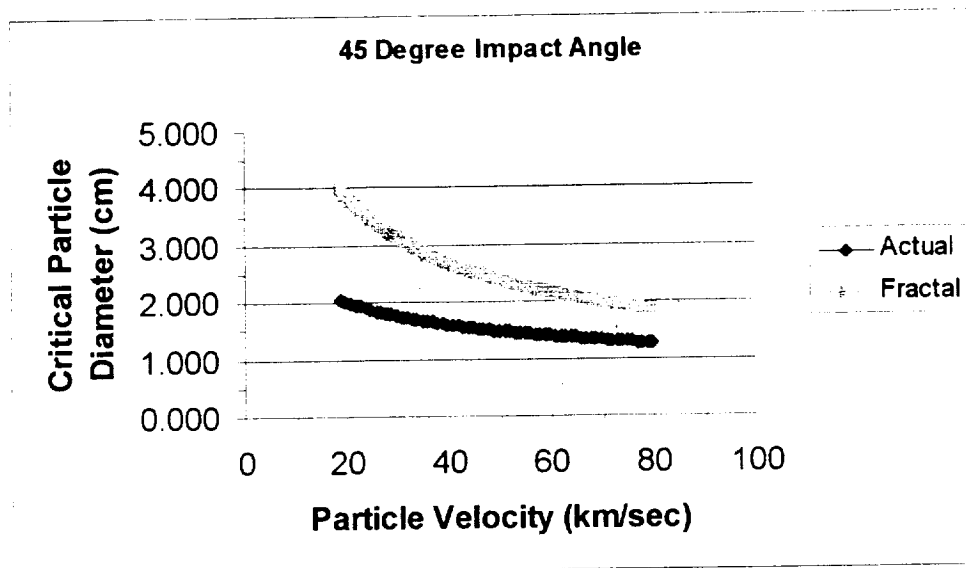


**Figure 2.3.5-4. Phenomenology Fractal for Stuffed Whipple Shield Configuration of ISS Propulsion Module in Meteoroid Environment (45 degree impact angle).
ISS Propulsion Module Parameters**

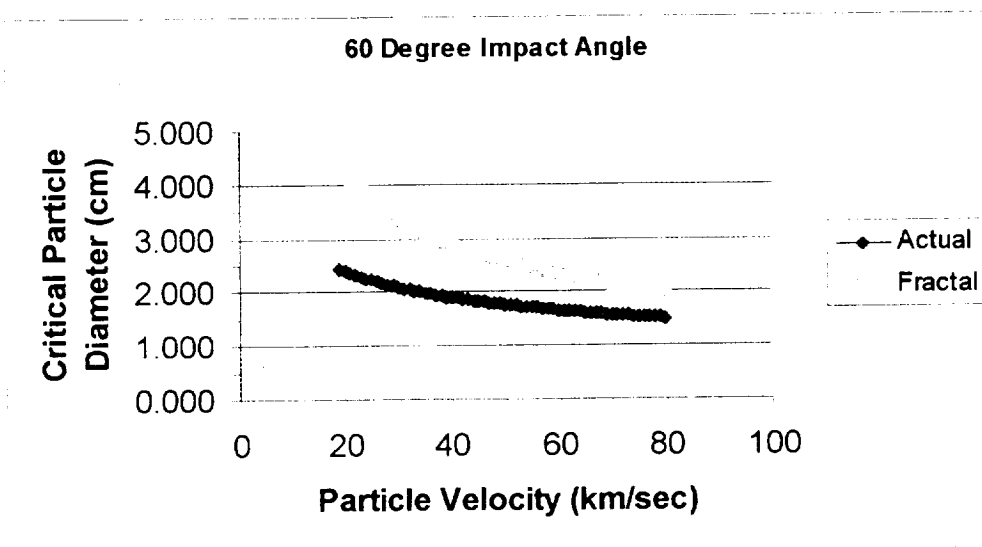


**Figure 2.3.5-5. Phenomenology Fractal for Stuffed Whipple Shield Configuration of ISS Propulsion Module in Meteoroid Environment (60 degree impact angle).
ISS Propulsion Module Parameters**

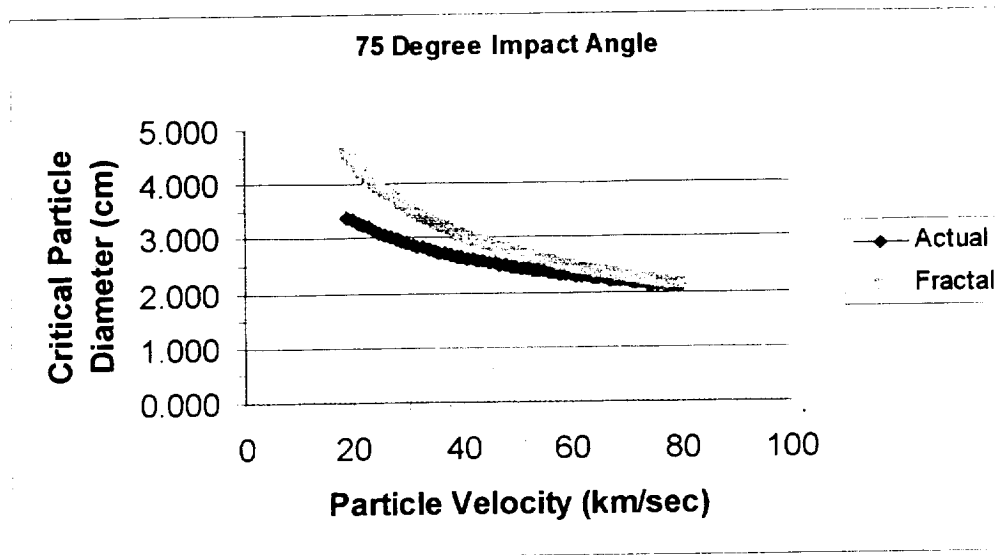


Figure 2.3.5-6. Phenomenology Fractal for Stuffed Whipple Shield Configuration of ISS Propulsion Module in Meteoroid Environment (75 degree impact angle).
ISS Propulsion Module Parameters

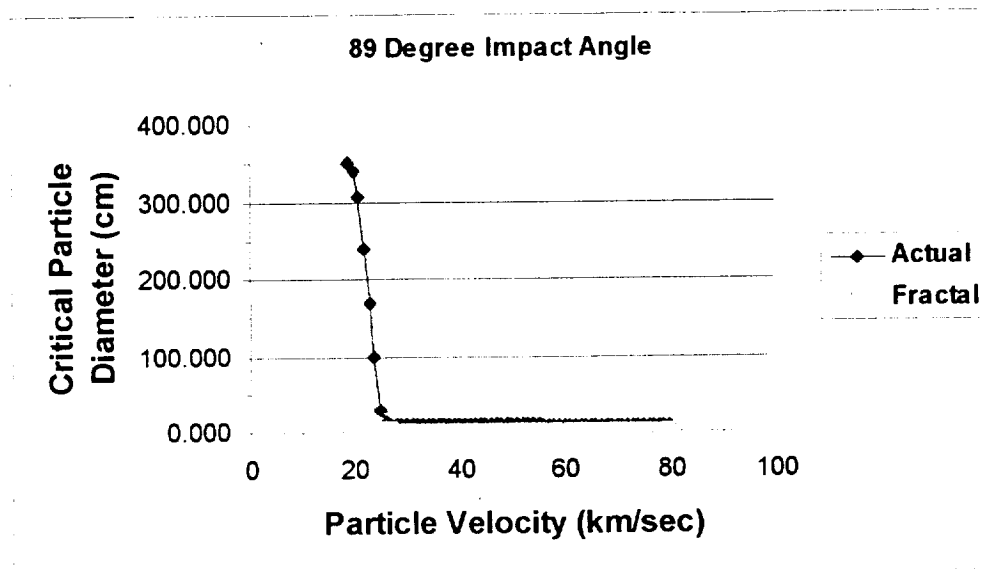


Figure 2.3.5-7. Phenomenology Fractal for Stuffed Whipple Shield Configuration of ISS Propulsion Module in Meteoroid Environment (90 degree impact angle).
ISS Propulsion Module Parameters

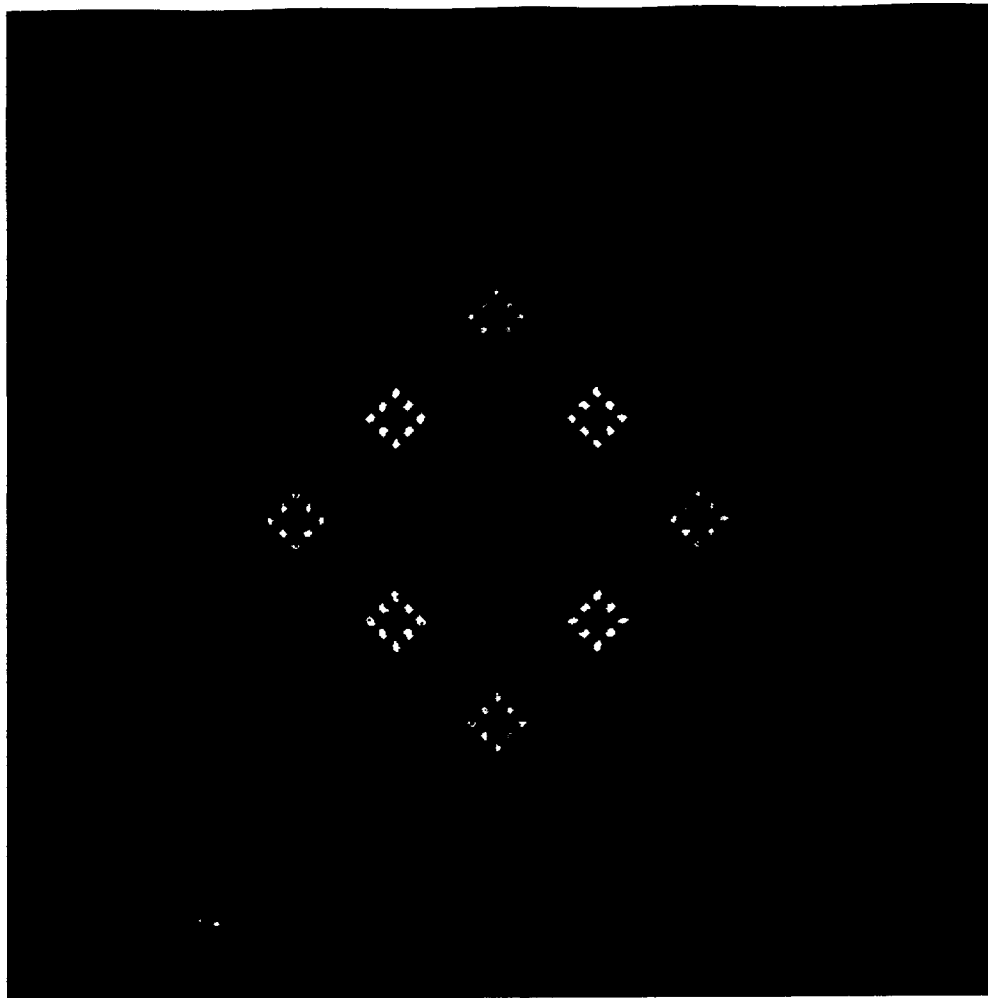


Figure 2.3.5-8. "Diamond Quilt" 2-D Fractal Representation of Stuffed Whipple Shield Phenomenology for Meteoroids Associated With ISS Propulsion Module at Altitude of 394.7 km (Dimension = 0.5319). Image created by replacing each line of a unit square by 3 lines, each 1/8 the length of the original, according to the formula $r = (N)^{1/D}$ where r = scaling factor (8), N = number of lines replacing original line (3), and D = dimension of fractal (0.5319). Error = 1.4%. (Image created using BRAZIL DESIGN software.)

2.4 Task 4: Comparison of Fractal Risk Assessment With BUMPER Results

The purpose of this task is to compare and contrast the fractal risk assessment of the ISS Propulsion Module with that provided by the BUMPER code and traditional spreadsheet risk assessment. The spreadsheet inputs and outputs are compared for consistency with the fractal approach. The fractal risk assessment is executed with consistency and completeness in mind. The results of the two methods (spreadsheet and fractal) are compared and contrasted statistically and qualitatively. Recommendations are made regarding improvements in the fractal approach. A “finite segment” analysis is performed using both spreadsheet and fractal methods, and producing a “risk plot,” showing the risk to orbital debris particles on the front face and sides of the Propulsion Module. This preliminary “risk plot” may be useful in comparison with equivalent BUMPER results.

2.4.1 Orbital Debris Risk Assessment - Whipple Shield Fractal Model

In this section, a risk assessment is performed for the ISS Propulsion Module with Whipple Shield configuration subject to the orbital debris environment with fixed particle density of 2.8 gm/cm^3 . Figure 2.4.1-1 shows the fit for the following “local” orbital debris flux fractal:

$$F_D(d) = 1.0509E - 04(d^{-1.4164})$$

This fractal was developed by considering the reduced range of values for critical orbital debris particle diameter pertinent to the Whipple Shield configuration of the ISS Propulsion Module. By considering only these particle diameters, a more accurate “local” orbital debris flux fractal can be obtained for analysis purposes. The correlation (R) for this fractal is 0.967, with significance level of $5.6E-36$, indicating an excellent statistical fit. (Note that all R values reported are for the $\ln(Y) = \ln(a) + b \ln(X)$ model, not for the $Y = a X^b$ model.)

The visual fit, while somewhat satisfactory could be improved by considering two ranges of particle diameters: above and below 1 cm, respectively. Nevertheless, we will see that the use of this fractal results in a high precision estimate of PNP, when compared to the equivalent traditional assessment.

Figure 2.4.1-2 shows the graphical representation of the local debris flux fractal. This fractal is obtained by replacing each line of a unit square by 7 lines, each $\frac{1}{4}$ the length of the original line. The figure shows only $\frac{1}{4}$ of the traditional “coastline” fractal for the debris flux. If, instead of replacing each line of the square, we replace the entire square by 7 squares, each $\frac{1}{4}$ the size of the original, we obtain the “gasket” fractal shown in Figure 2.4.1-3.

Figure 2.4.1-4 shows the fit for the following “non-fractal” approximating model to the orbital debris velocity probability distribution:

$$f'(V) = 8.177E - 04(V^{1.4172})$$

While the correlation (R) to the actual model of 0.985 is statistically significant (1.3E-45), the visual fit for this model leaves something to be desired. Nevertheless, we will see that employing this model in the integrated analysis is satisfactory for this particular situation.

Integration:

We first combine the Whipple Shield Phenomenology fractal

$$D_{crit} = 2.917V^{-0.6028}$$

with the local orbital debris flux fractal

$$F_D(d) = 1.0509E - 04(d^{-1.4164})$$

to obtain the following (setting $d = D_{crit}$):

$$\begin{aligned} F_D(V) &= 1.0509E - 04[2.917(V^{-0.6028})]^{-1.4164} \\ &= 2.3069E - 05(V^{0.8538}) \end{aligned}$$

Next, we multiply this by the approximating model for orbital debris velocity probability distribution:

$$\begin{aligned} f'(V)F_D(V) &= 8.177E - 04(V^{1.4172})2.3069E - 05(V^{0.8538}) \\ &= 1.8863E - 08(V^{2.271}) \end{aligned}$$

Now, we can calculate the ISS Propulsion Module orbital debris PNP for an effective area of 63.94 m² as:

$$PNP_{Debris} = e^{-63.94(4.244) \int_0^{15} 1.8863E-08(V^{2.271})dV}$$

$$= e^{-5.1187E-06(\frac{15^{3.271}}{3.271})} = e^{-1.1E-02} = 0.9891$$

Note that the factor of 4.244 in front of the integral is necessary to guarantee that:

$$4.244 \int_0^{15} f'(V)dV = 1$$

The upper limit of both integrals corresponds to the highest (non-zero) velocity value for orbital debris particles for the situation analyzed. The equivalent orbital debris PNP using traditional risk assessment is 0.9876, resulting in a relative difference of 0.15%.

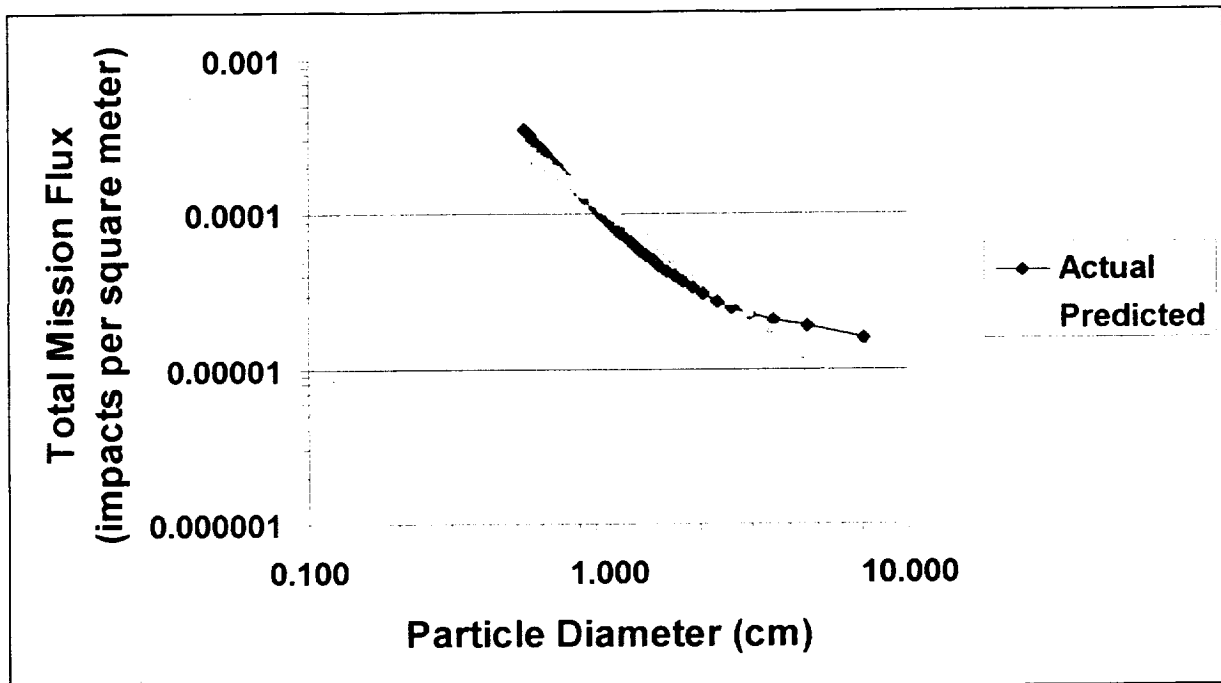


Figure 2.4.1-1. Local Orbital Debris Flux Fractal for Relevant Whipple Shield Particle Diameters. Fractal Model is “Predicted.” ISS Propulsion Module Parameters (Orbital debris particles greater than 10 cm are tracked and avoided.)

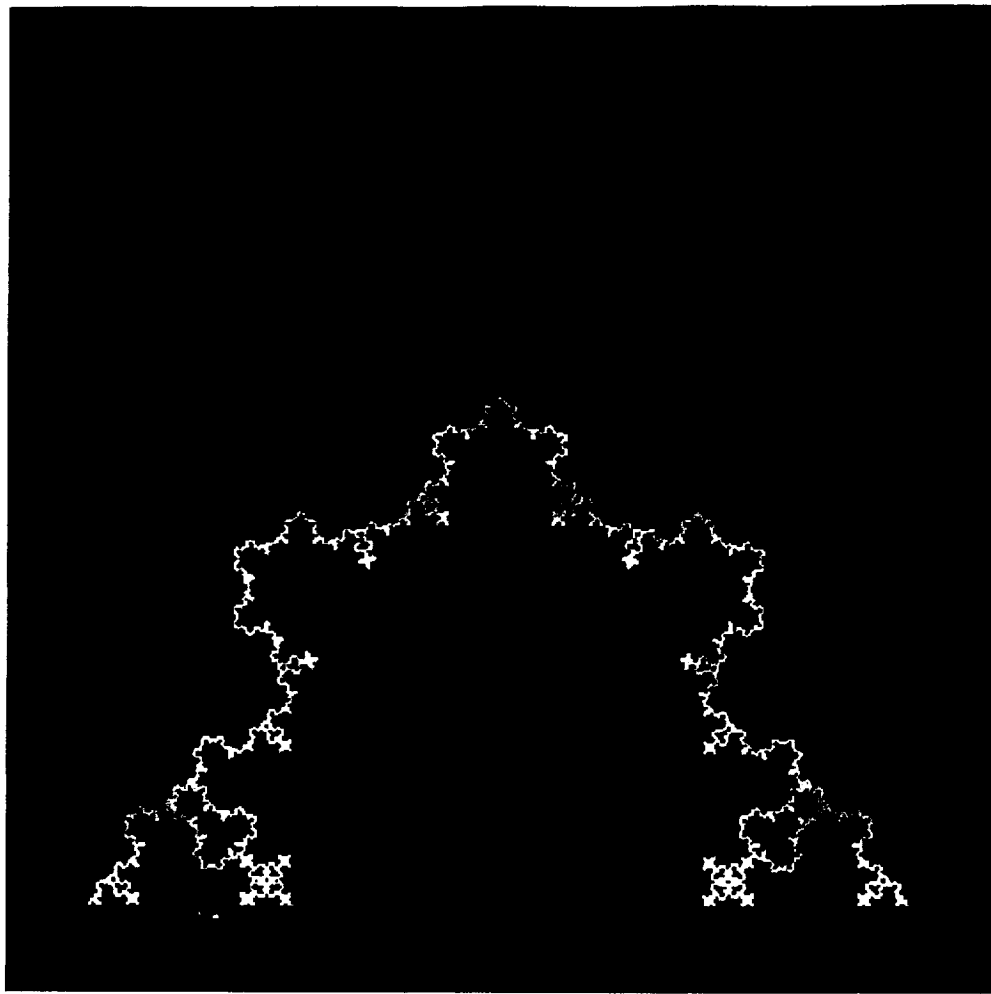


Figure 2.4.1-2. "Inimitable Lightning" 2-D Fractal Representation of Whipple Shield Pertinent Orbital Debris Flux for ISS Propulsion Module at Altitude of 394.7 km (Dimension = 1.4164). Image created by replacing each line of a unit square by 7 lines, each 1/4 the length of the original, according to the formula $r = (N)^{1/D}$ where r = scaling factor (4), N = number of lines replacing original line (7), and D = dimension of fractal (1.4164). Error = 1.3%. (Image created using BRAZIL DESIGN software.)

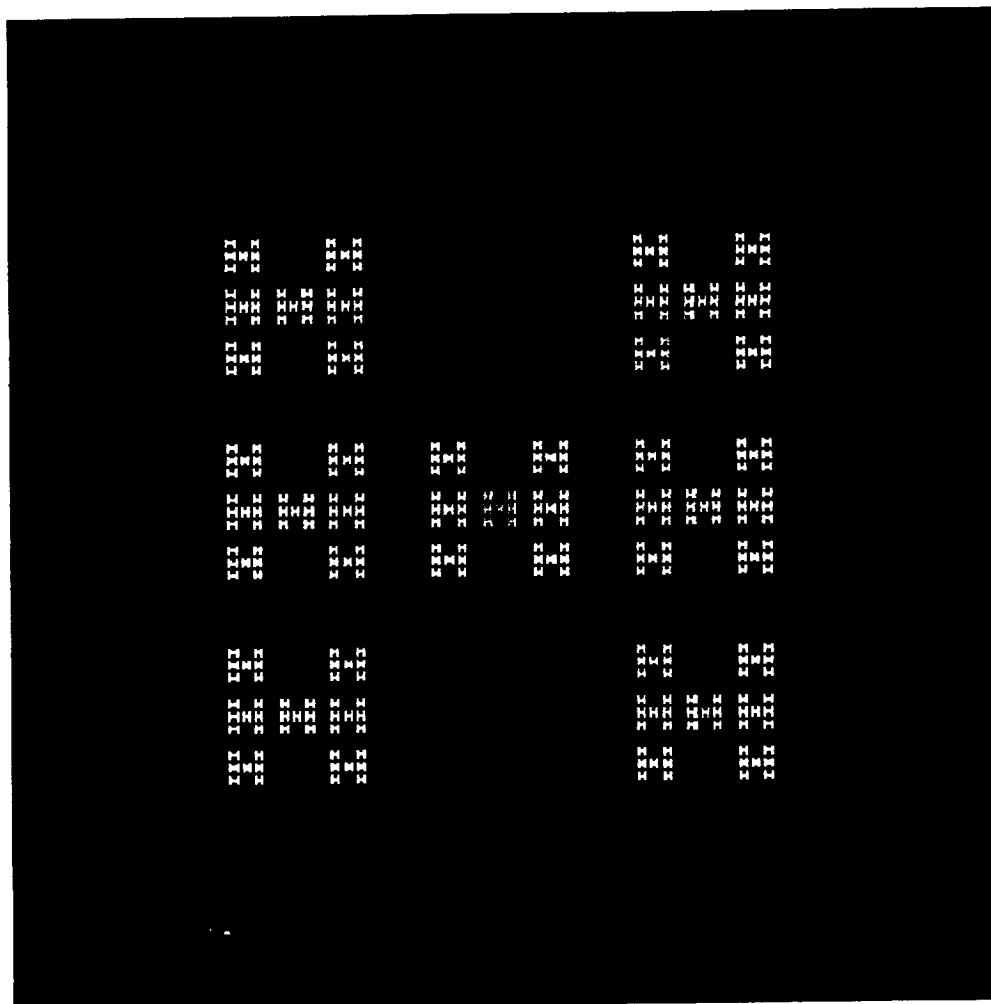


Figure 2.4.1-3. "ISS H-Dmg" 2-D "Gasket" Fractal Representation of Whipple Shield Pertinent Orbital Debris Flux for ISS Propulsion Module at Altitude of 394.7 km (Dimension = 1.4164). Image created by replacing each unit square by 7 squares, each 1/4 the size of the original, according to the formula $r = (N)^{1/D}$ where r = scaling factor (4), N = number of squares replacing original square (7), and D = dimension of fractal (1.4164). Error = 1.3%. (Image created using BRAZIL DESIGN software.)

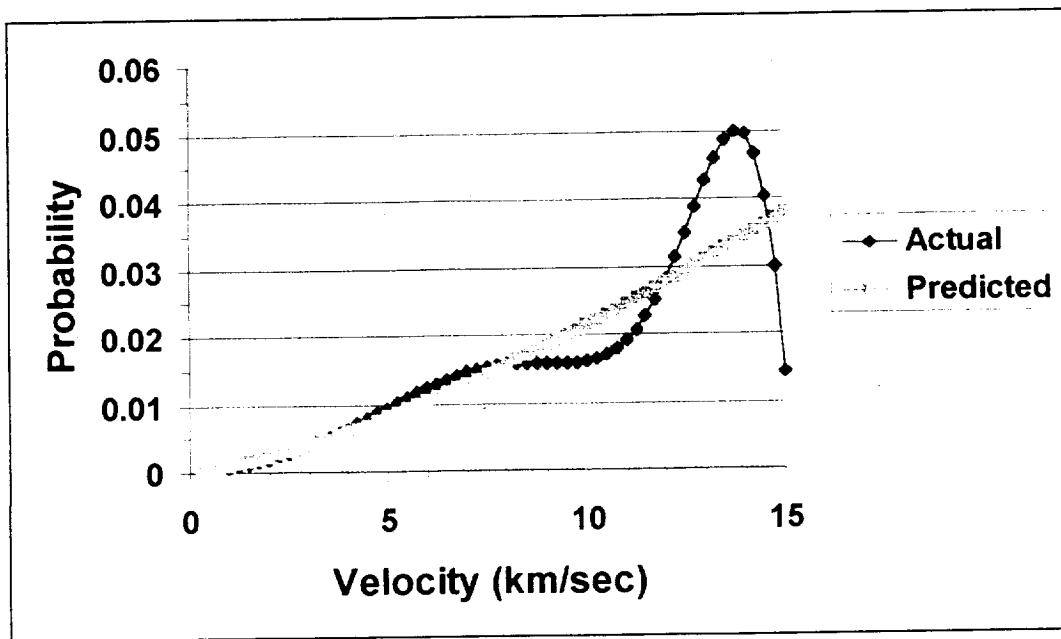


Figure 2.4.1-4. Approximating “Non-Fractal” Model for Orbital Debris Velocity Probability Distribution. ISS Propulsion Module Parameters

2.4.2 Orbital Debris Risk Assessment - Stuffed Whipple Shield Fractal Model

In this section, a risk assessment is performed for the ISS Propulsion Module with Stuffed Whipple Shield configuration subject to the orbital debris environment with fixed particle density of 2.8 gm/cm^3 . Figure 2.4.2-1 shows the fit for the following “local” orbital debris flux fractal:

$$F_D(d) = 8.4784E - 05(d^{-1.0626})$$

This fractal was developed by considering the reduced range of values for orbital debris critical particle diameter pertinent to the Stuffed Whipple Shield configuration of the ISS Propulsion Module. By considering only these particle diameters, a more accurate “local” orbital debris flux fractal can be obtained for analysis purposes. The correlation (R) for this fractal is 0.931, with significance level of $6.8E-28$, indicating an excellent statistical fit. (Note that all R values reported are for the $\ln(Y) = \ln(a) + b \ln(X)$ model, not for the $Y = a X^b$ model.)

The visual fit, while somewhat satisfactory could be improved by considering two ranges of particle diameters: above and below 300 cm, respectively. Nevertheless, we will see that the use of this fractal results in a high precision estimate of PNP, when compared to the equivalent traditional assessment.

Figure 2.4.2-2 shows the graphical representation of the local debris flux fractal. This fractal is obtained by replacing each line of a unit square by 8 lines, each 1/7 the length of the original line. The figure shows only 1/4 of the traditional “coastline” fractal for the debris flux. The relative smoothness of this fractal is indicative of a dimension in the vicinity of 1.0 (actual fractal dimension = 1.0626).

Integration:

We first combine the Stuffed Whipple Shield Phenomenology fractal

$$D_{crit} = 86.73V^{-1.789}$$

with the local orbital debris flux fractal

$$F_D(d) = 8.4784E-05(d^{-1.0626})$$

to obtain the following (setting $d = D_{crit}$):

$$\begin{aligned} F_D(V) &= 8.4784E-05[86.73(V^{-1.789})]^{-1.0626} \\ &= 7.3929E-07(V^{1.901}) \end{aligned}$$

Next, we multiply this by the approximating model for orbital debris velocity probability distribution:

$$\begin{aligned} f'(V)F_D(V) &= 8.177E-04(V^{1.4172})7.3929E-07(V^{1.901}) \\ &= 6.0452E-10(V^{3.318}) \end{aligned}$$

Now, we can calculate the ISS Propulsion Module orbital debris PNP for an effective area of 63.94 m² as:

$$\begin{aligned} PNP_{Debris} &= e^{-63.94(4.244) \int_0^{15} 6.0452E-10(V^{3.318})dV} \\ &= e^{-1.6404E-07(\frac{15^{4.318}}{4.318})} = e^{-4.55E-03} = 0.9955 \end{aligned}$$

Note that the factor of 4.244 in front of the integral is necessary to guarantee that:

$$4.244 \int_0^{15} f'(V) dV = 1$$

The upper limit of both integrals corresponds to the highest (non-zero) velocity value for orbital debris particles for the situation analyzed. The equivalent orbital debris PNP using traditional risk assessment is 0.9965, resulting in a relative difference of 0.10%.

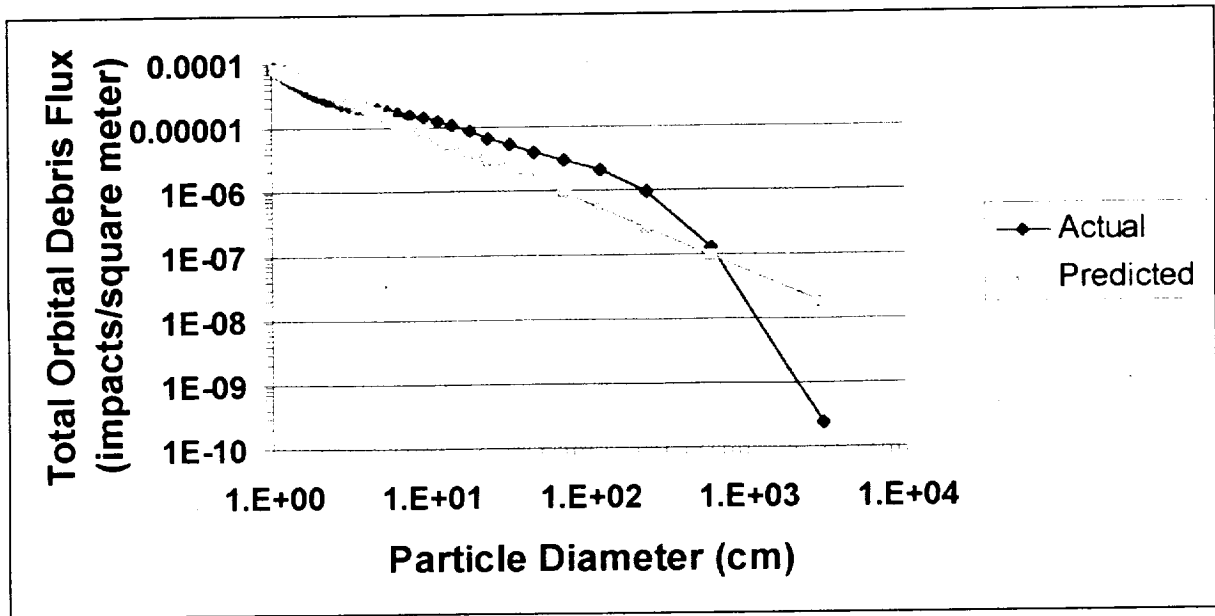


Figure 2.4.2-1. Local Orbital Debris Flux Fractal for Relevant Stuffed Whipple Shield Particle Diameters. Fractal Model is "Predicted." ISS Propulsion Module Parameters (Orbital debris particles greater than 10 cm are tracked and avoided.)

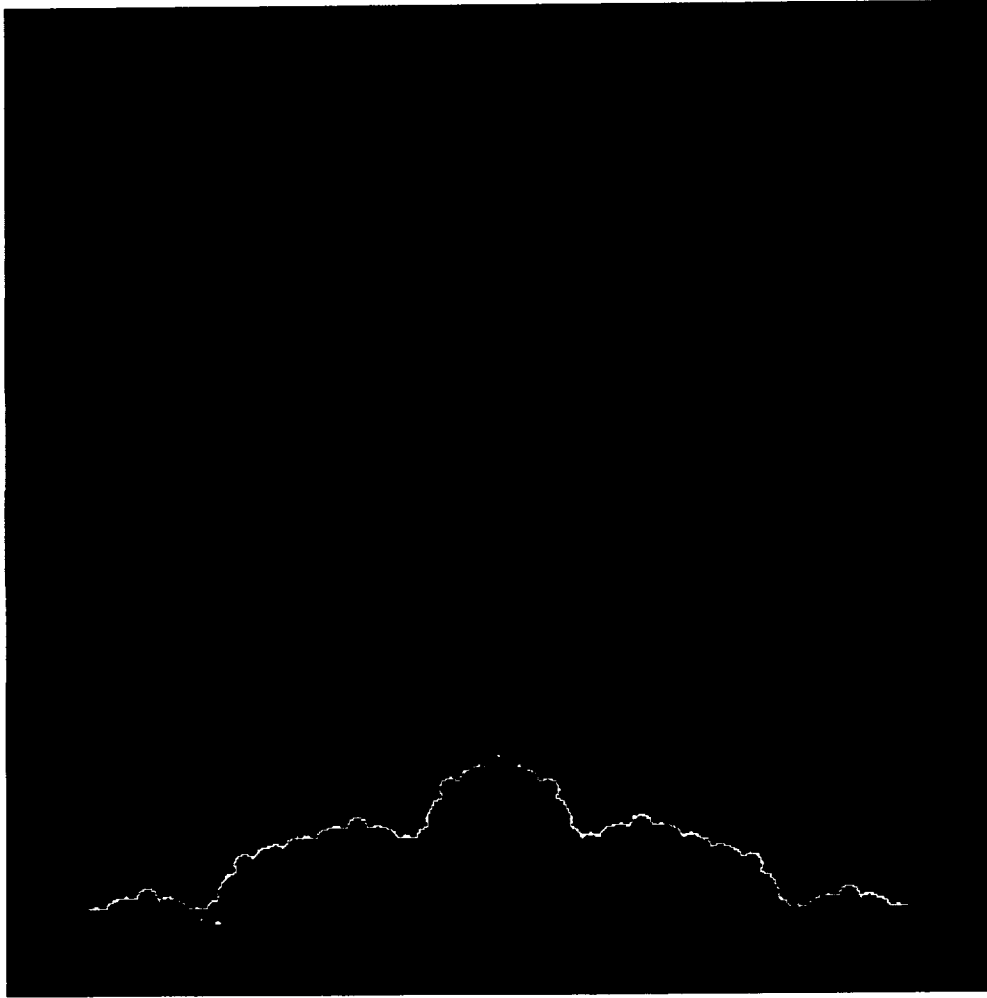


Figure 2.4.2-2. “Rolling Hills” 2-D Fractal Representation of Stuffed Whipple Shield Pertinent Orbital Debris Flux for ISS Propulsion Module at Altitude of 394.7 km (Dimension = 1.0626). Image created by replacing each line of a unit square by 8 lines, each 1/7 the length of the original, according to the formula $r = (N)^{1/D}$ where r = scaling factor (7), N = number of lines replacing original line (8), and D = dimension of fractal (1.0626). Error = 1.1%. (Image created using BRAZIL DESIGN software.)

2.4.3 Meteoroid Risk Assessment - Whipple Shield Fractal Model

In this section, a risk assessment is performed for the ISS Propulsion Module with Whipple Shield configuration subject to the meteoroid environment. Figure 2.4.3-1 shows the fit for the following “local” meteoroid flux fractal:

$$F_M(d) = 6.357E - 06(d^{-3.333})$$

This fractal was developed by considering the reduced range of values for critical meteoroid particle diameter pertinent to the Whipple Shield configuration of the ISS Propulsion Module. By considering only these particle diameters, a more accurate "local" meteoroid flux fractal can be obtained for analysis purposes. The correlation (R) for this fractal is 0.985, with significance level of <1E-235, indicating an excellent statistical fit. (Note that all R values reported are for the $\ln(Y) = \ln(a) + b \ln(X)$ model, not for the $Y = a X^b$ model.) Note that the impact angle is not a significant predictor variable for this model.

Figure 2.4.3-2 shows the graphical representation of the local meteoroid flux fractal. This fractal is obtained by replacing each line of a unit square by 10 lines, each 1/2 the length of the original line. The figure shows only 1/4 of the traditional "coastline" fractal for the meteoroid flux. It is very difficult to obtain a meaningful 2-D representation of a greater-than-3-D fractal.

Figure 2.4.3-3 shows the fit for the following fractal model to the meteoroid velocity probability distribution:

$$f'(V) = 2.653E-06(V^{-5.56})$$

The correlation (R) to the actual model of 0.986 is statistically significant (<1E-235), and the visual fit for this model is quite good. Furthermore, we will see that employing this model in the integrated analysis is satisfactory for this particular situation. No meaningful fractal 2-D graphical representation can be made for a fractal with dimension greater than 5.

Integration:

We first combine the Whipple Shield Phenomenology fractal

$$D_{crit} = 7.016V^{-0.8143}(\theta + 1)^{0.1595}$$

with the local meteoroid flux fractal

$$F_M(d) = 6.357E-06(d^{-3.333})$$

to obtain the following (setting $d = D_{crit}$):

$$\begin{aligned} F_M(V, \theta) &= 6.357E-06[7.016(V^{-0.8143})(\theta + 1)^{0.1595}]^{-3.333} \\ &= 9.62E-09(V^{2.714})(\theta + 1)^{-0.5316} \end{aligned}$$

Next, we multiply this by the fractal model for meteoroid velocity probability distribution:

$$\begin{aligned} f'(V)F_M(V, \theta) &= 2.653E+06(V^{-5.56})9.62E-09(V^{2.714})(\theta+1)^{-0.5316} \\ &= 2.552E-02(V^{-2.846})(\theta+1)^{-0.5316} \end{aligned}$$

Now, we can calculate the ISS Propulsion Module meteoroid PNP for an effective area of 40.65 m² as:

$$\begin{aligned} PNP_{Meteoroid} &= e^{-40.65\left(\frac{1}{81}\right) \int_0^{90} \int_{18.8}^{79.8} 2.552E-02(V^{-2.846})(\theta+1)^{-0.5316} dV d\theta} \\ &= e^{-4.456E-04} = 0.99955 \end{aligned}$$

Note that the factor of 1/81 in front of the integral is necessary to guarantee that:

$$\frac{1}{81} \int_0^{90} \int_{18.8}^{79.8} f'(V) dV d\theta = 1$$

The equivalent meteoroid PNP using traditional risk assessment is 0.9993, resulting in a relative difference of +0.025%.

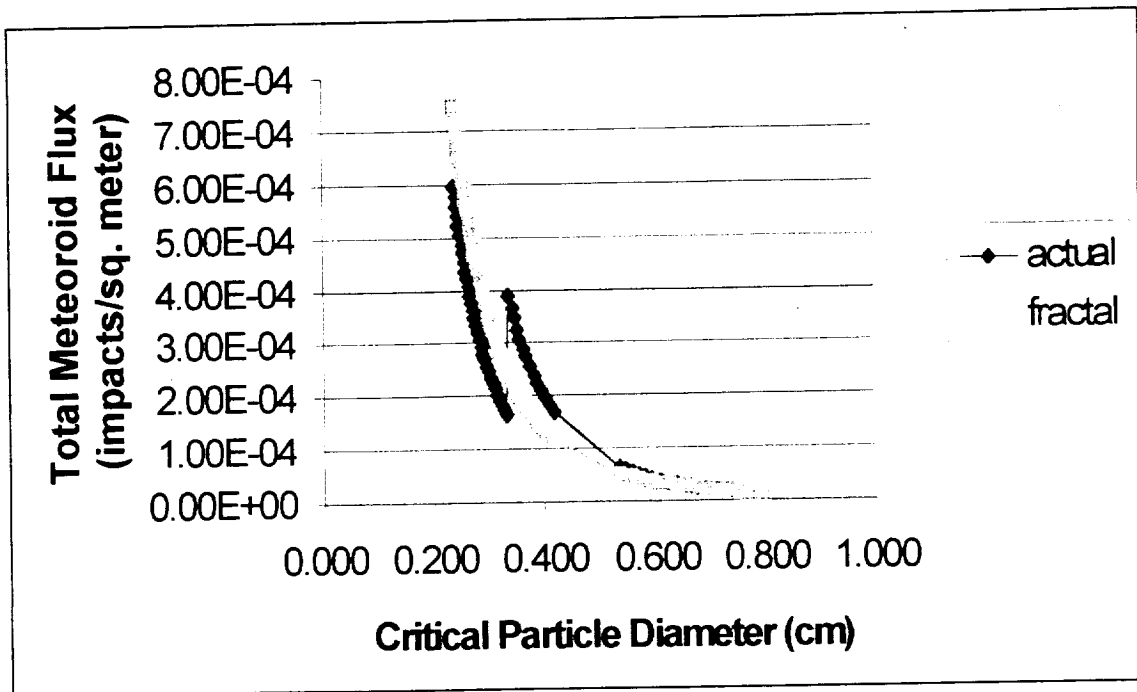


Figure 2.4.3-1. Local Meteoroid Flux Fractal for Relevant Whipple Shield Particle Diameters. Fractal Model is "Predicted." ISS Propulsion Module Parameters (Meteoroid particles greater than 10 cm are tracked and avoided.)

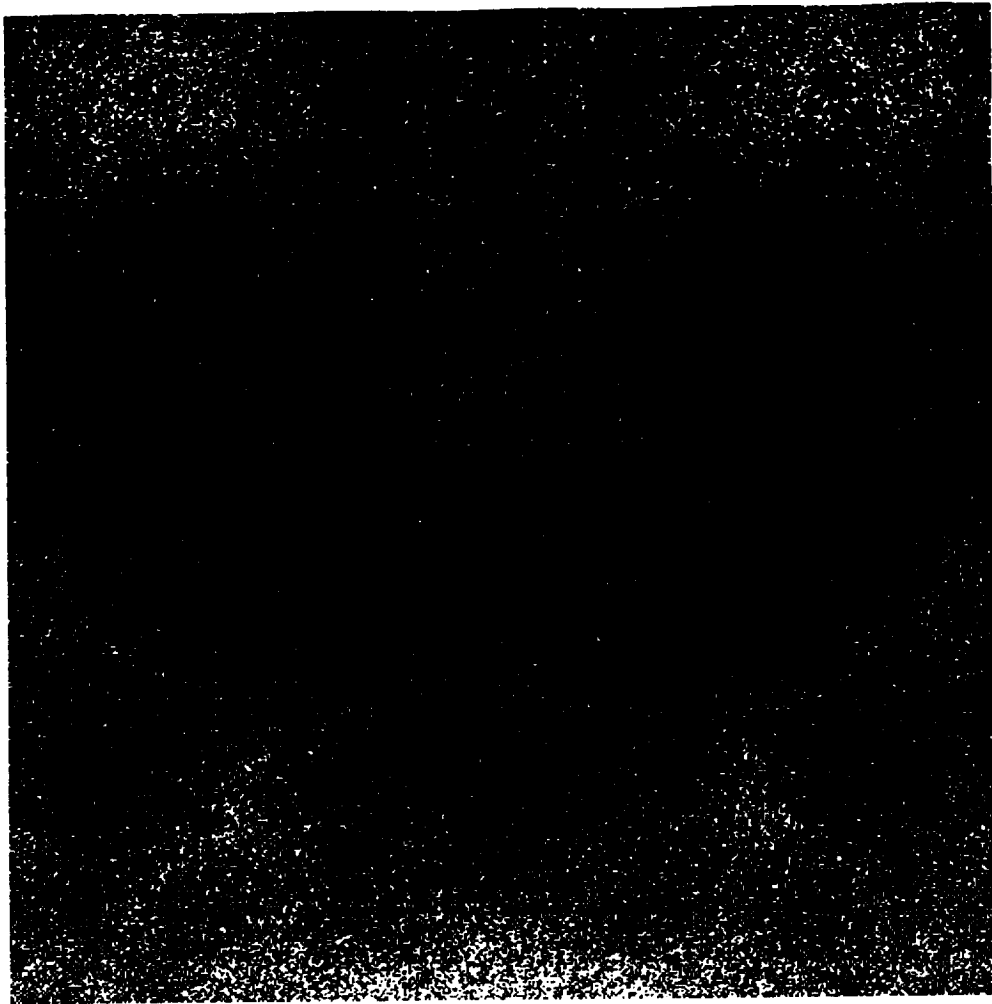


Figure 2.4.3-2. "Abstract Space" 2-D Fractal Representation of Whipple Shield Pertinent Meteoroid Flux for ISS Propulsion Module at Altitude of 394.7 km (Dimension = 3.333). Image created by replacing each line of a unit square by 10 lines, each 1/2 the length of the original, according to the formula $r = (N)^{1/D}$ where r = scaling factor (2), N = number of lines replacing original line (10), and D = dimension of fractal (3.3333). Error = 0.25%. (Image created using BRAZIL DESIGN software.)

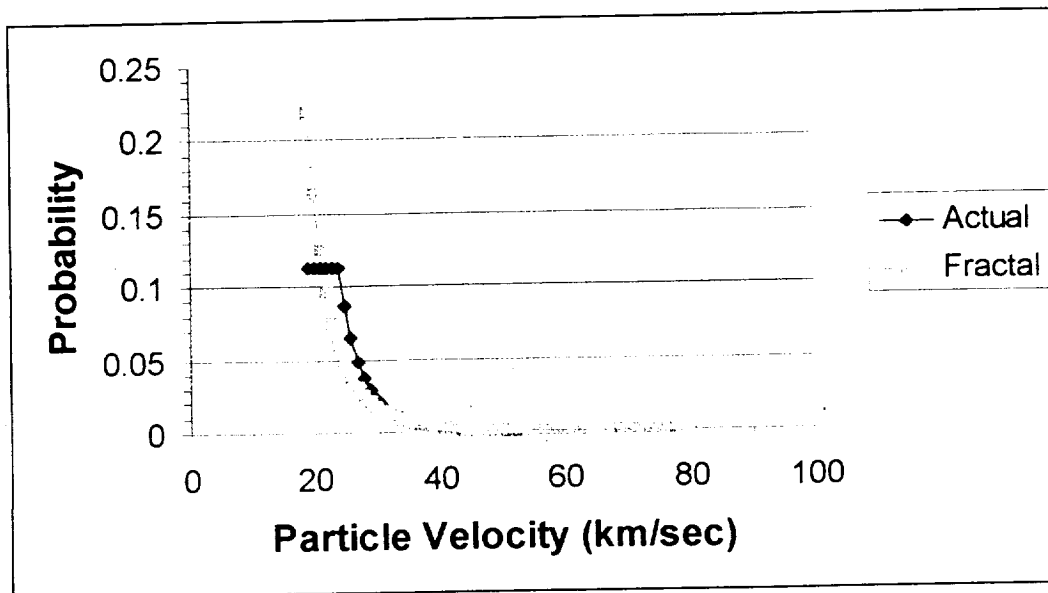


Figure 2.4.3-3. Fractal Model for Meteoroid Velocity Probability Distribution.
ISS Propulsion Module Parameters

2.4.4 Meteoroid Risk Assessment - Stuffed Whipple Shield Fractal Model

In this section, a risk assessment is performed for the ISS Propulsion Module with Stuffed Whipple Shield configuration subject to the meteoroid. Figure 2.4.4-1 shows the fit for the following “local” meteoroid flux fractal:

$$F_M(d) = 5.320E-06(d^{-4.0097})$$

This fractal was developed by considering the reduced range of values for meteoroid critical particle diameter pertinent to the Stuffed Whipple Shield configuration of the ISS Propulsion Module. By considering only these particle diameters, a more accurate “local” meteoroid flux fractal can be obtained for analysis purposes. The correlation (R) for this fractal is 1.0, with significance level of 0.0, indicating an excellent statistical fit. (Note that all R values reported are for the $\ln(Y) = \ln(a) + b \ln(X)$ model, not for the $Y = a X^b$ model.)

No graphical representation is provided for two reasons. The first is that this “fractal” has almost integer dimension. The second reason is that the dimension is much higher than a 2-D representation could capture.

Integration:

We first combine the Stuffed Whipple Shield Phenomenology fractal

$$D_{crit} = 6.81V^{-0.5319}(\theta + 1)^{0.2679}$$

with the local meteoroid flux fractal

$$F_M(d) = 5.320E-06(d^{-4.0097})$$

to obtain the following (setting $d = D_{crit}$):

$$\begin{aligned} F_M(V, \theta) &= 5.320E-06[6.81(V^{-0.5319})(\theta + 1)^{0.2679}]^{-4.0097} \\ &= 2.4281E-09(V^{2.133})(\theta + 1)^{-1.0742} \end{aligned}$$

Next, we multiply this by the fractal model for meteoroid velocity probability distribution:

$$\begin{aligned} f'(V)F_M(V, \theta) &= 2.653E+06(V^{-5.56})2.4281E-09(V^{2.133})(\theta + 1)^{-1.0742} \\ &= 6.442E-03(V^{-3.427})(\theta + 1)^{-1.0742} \end{aligned}$$

Now, we can calculate the ISS Propulsion Module meteoroid PNP for an effective area of 40.65 m² as:

$$\begin{aligned} PNP_{Meteoroid} &= e^{-40.65(\frac{1}{81}) \int_0^{90} \int_{18.8}^{79.8} 6.442E-03(V^{-3.427})(\theta+1)^{-1.0742} dVd\theta} \\ &= e^{-3.9143E-06} = 0.9999960 \end{aligned}$$

Note that the factor of 1/81 in front of the integral is necessary to guarantee that:

$$\frac{1}{81} \int_0^{90} \int_{18.8}^{79.8} f'(V) dV d\theta = 1$$

The equivalent meteoroid PNP using traditional risk assessment is 0.999982, resulting in a relative difference of +0.0014%.

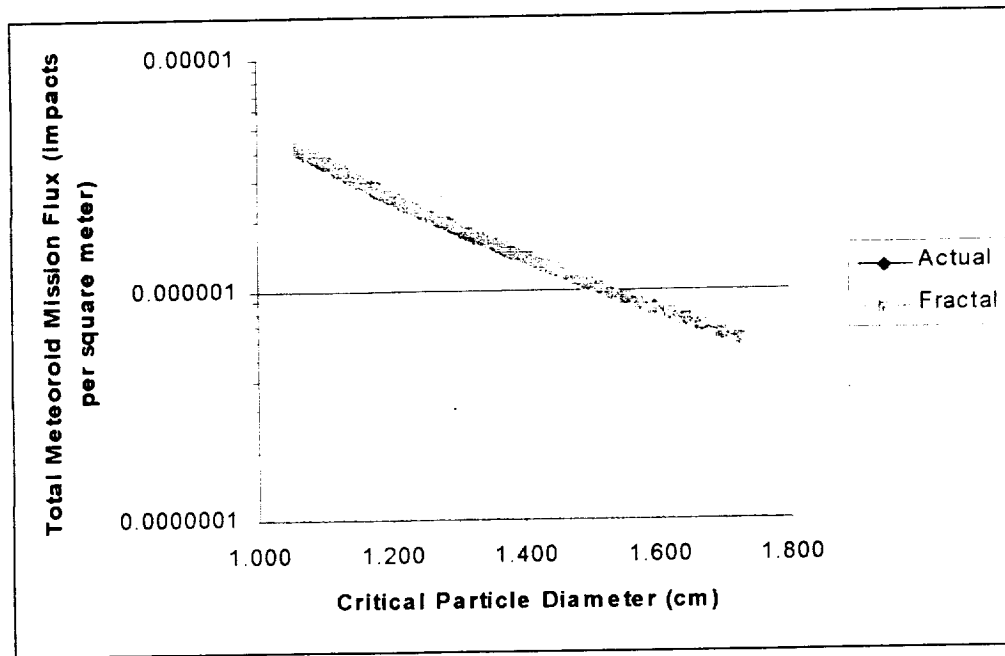


Figure 2.4.4-1. Local Meteoroid Flux Fractal for Relevant Stuffed Whipple Shield Particle Diameters. Fractal Model is “Predicted.” ISS Propulsion Module Parameters

2.4.5 Fractal Morphological Studies

Figure 2.4.5-1 shows a “morphing” transformation from the global orbital debris fractal (dimension = 2.1308) to the local orbital debris fractal (dimension = 1.4164) pertinent to the Whipple shield configuration of the ISS Propulsion Module. Given that this transformation occurs from a greater-than-2-D fractal to a lesser-than-2-D fractal, it seems reasonable that the global orbital debris fractal would need to “lose” some density. This density loss is evident in the second frame, and by the third and fourth frames, Ford [2001] observed that the mass making its way down from the center of the fractal is composed of images self-similar to the overall dynamic fractal. Furthermore, Ford has observed that the self-similarity continues “back” into the larger portion of the fractal in a number of directions, and that the mass breaking off tends toward the lower right portion of the destination (local debris) fractal. While this transformation is not entirely symmetrical in nature, these observations do lead one to conclude that the dynamics of morphing can be carried out with as much self-similarity as possible.

Figure 2.4.5-2 shows a morphing transformation from the global meteoroid fractal (dimension = 1.1782) to the phenomenology meteoroid fractal (dimension = 0.8143) for the Whipple Shield configuration of the ISS Propulsion Module. Because these dimensions are “closer” than those for the previous morphological study, it might be expected that less mass would need to be lost from the initial fractal to achieve the destination fractal. Again, it is evident by the third or fourth frame that this dynamic process is taking place in a self-similar fashion.

Morphing Global Orbital Debris to Local Debris (Whipple)

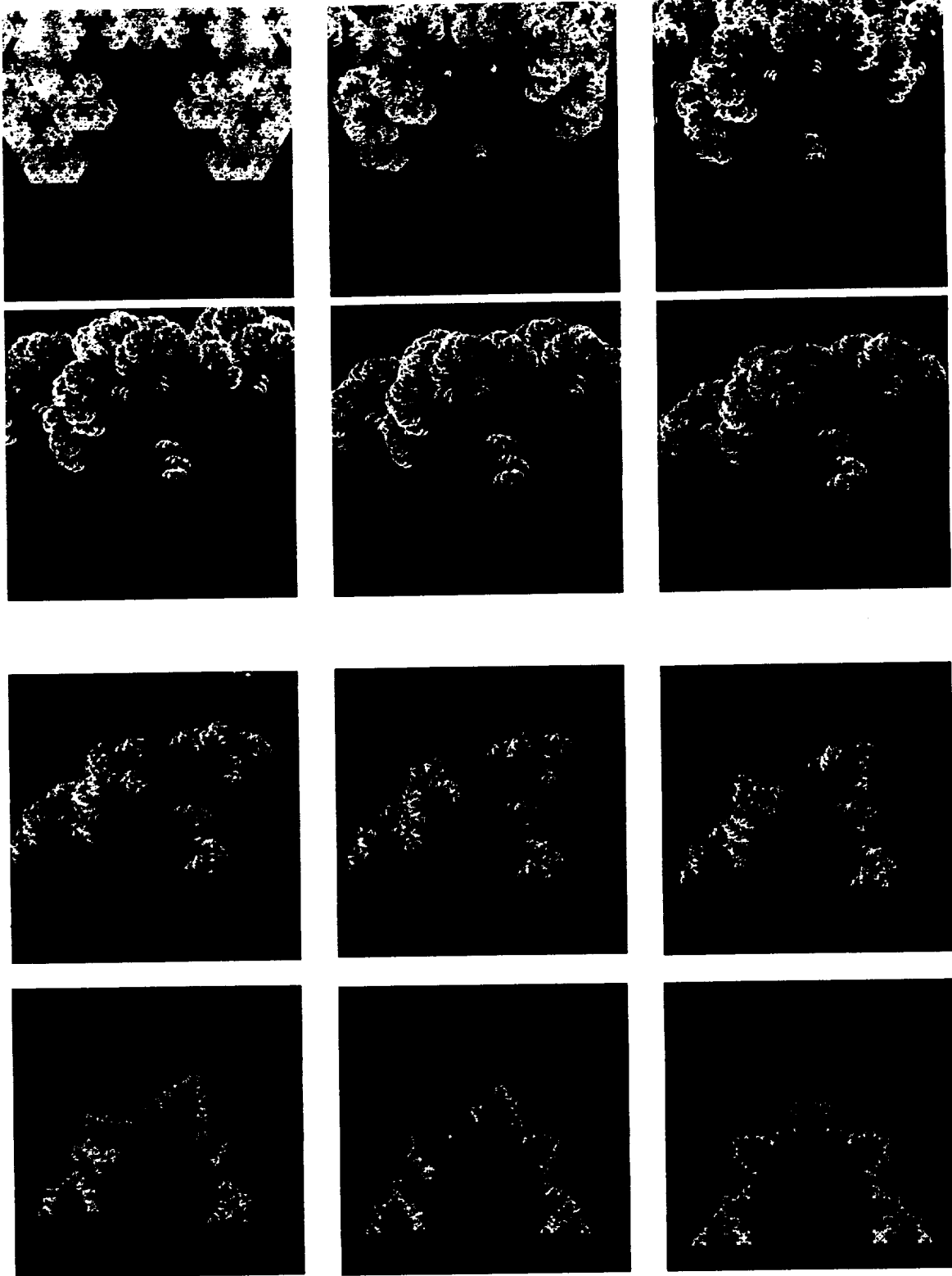
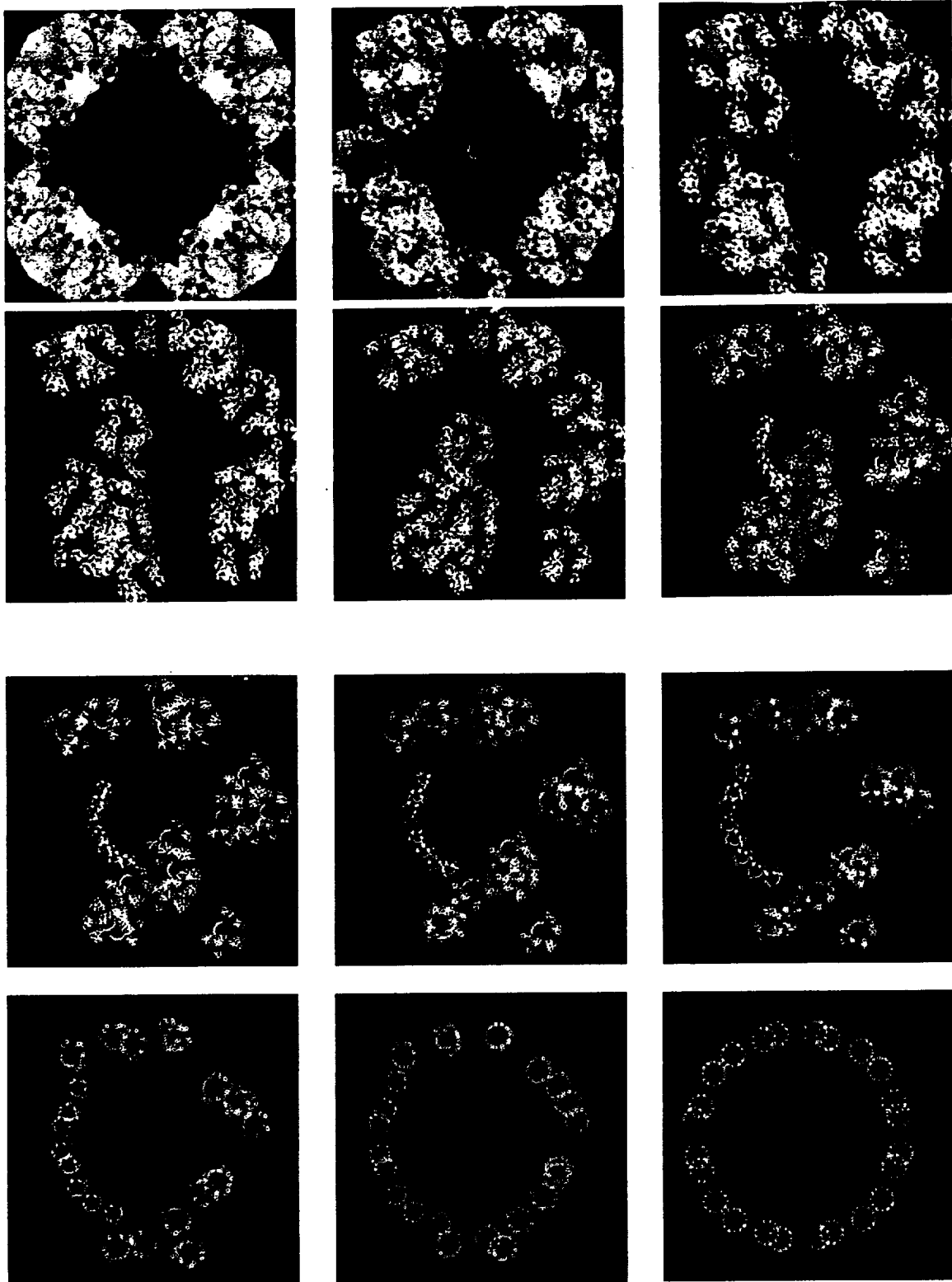


Figure 2.4.5-1. Transformation of Global Orbital Debris Fractal to Local (Whipple) Orbital Debris Fractal



**Figure 2.4.5-2. Transformation of Global Meteoroid Fractal to Phenomenology
(Whipple) Meteoroid Fractal**

2.4.6 “Finite Segment” Orbital Debris Risk Assessment - Stuffed Whipple Shield

In this section, a “finite segment” representation of the ISS Propulsion Module has been approximated for the Stuffed Whipple Shield configuration subjected to orbital debris impacts. The analysis has been performed using an innovative spreadsheet approach to the traditional risk assessment, as well as an analogous fractal methodology.

The approach used is to segment the ISS Propulsion Module in an angular fashion around the circumference of the cylindrical portion. Critical particle diameters are then calculated for each segment of the cylinder. These critical particle diameters depend on one of two dominating impact angles. Figure 2.4.6-1 provides a sketch of these considerations.

Figure 2.4.6-2 shows the “thermal” plot of the front and side views of the ISS Propulsion Module for the traditional risk assessment. The redder areas correspond to those areas or segments with lower relative PNP estimates, and thus, higher risk. The lighter yellow areas near the top and bottom of the Module reflect higher PNP estimates, and thus, lower risk. As expected, the front surface and angular segments near the center of the Module’s side have greater risk estimates. It is important to note that the radial symmetry of risk assessment is due to a lack of consideration of self-shadowing and shadowing by other ISS Elements. Thus, this “finite segment” approach is a first approximation to the ISS Propulsion Module risk assessment.

The overall PNP estimate using the “finite segment” approach is 0.9962, as compared to 0.9965 for the “global” traditional risk assessment.

Figure 2.4.6-3 shows the “thermal” plot of the front and side views of the ISS Propulsion Module for the fractal risk assessment. To create this plot, fractal models were created for the RAM face, and each of the angular segments around the circumference of the cylindrical portion of the ISS Propulsion Module. These fractal models were then used to calculate PNP’s in a similar fashion as for the “global” assessments described in previous sections.

In Figure 2.4.6-3, the redder areas again correspond to those areas or segments with lower relative PNP estimates, and thus, higher risk. The lighter yellow areas near the top and bottom of the Module reflect higher PNP estimates, and thus, lower risk. As expected, the front surface and angular segments near the center of the Module’s side have greater risk estimates. It is important to note that the radial symmetry of risk assessment is due to a lack of consideration of self-shadowing and shadowing by other ISS Elements. Thus, this “finite segment” approach is a first approximation to the ISS Propulsion Module risk assessment.

The overall PNP estimate using the “finite segment” approach is 0.9955, identical to that for the “global” fractal risk assessment.

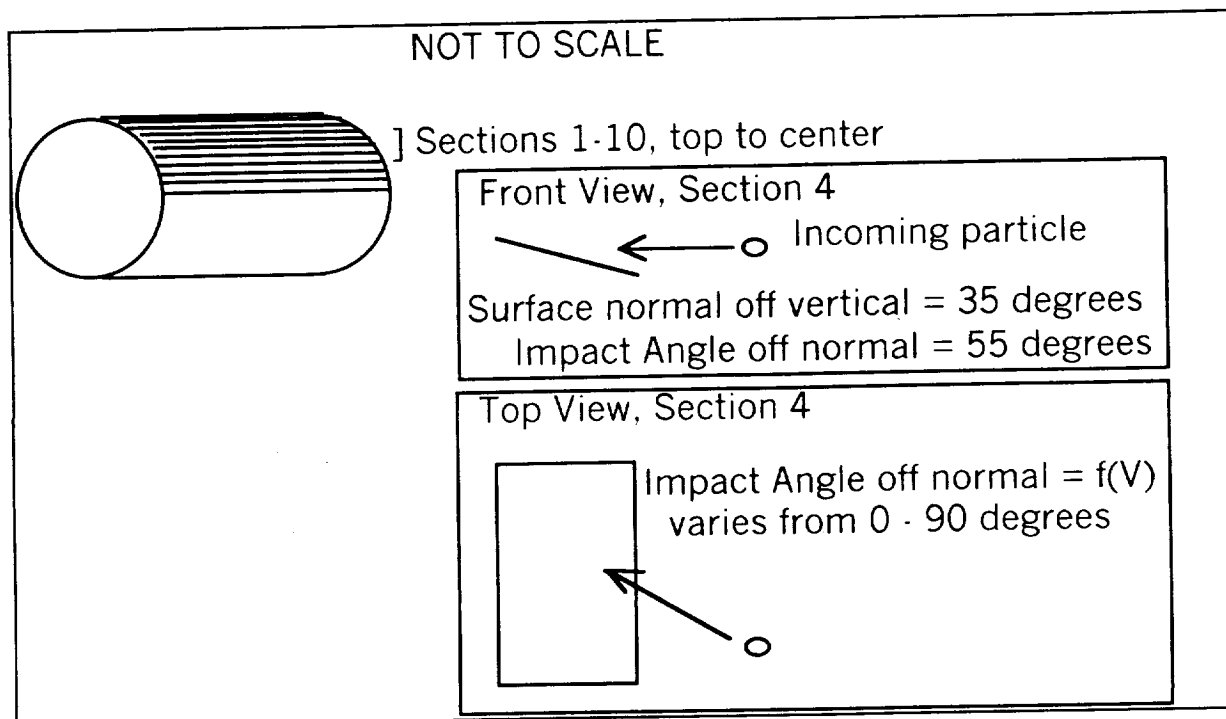


Figure 2.4.6-1. Sketch of "Finite Segment" Approach

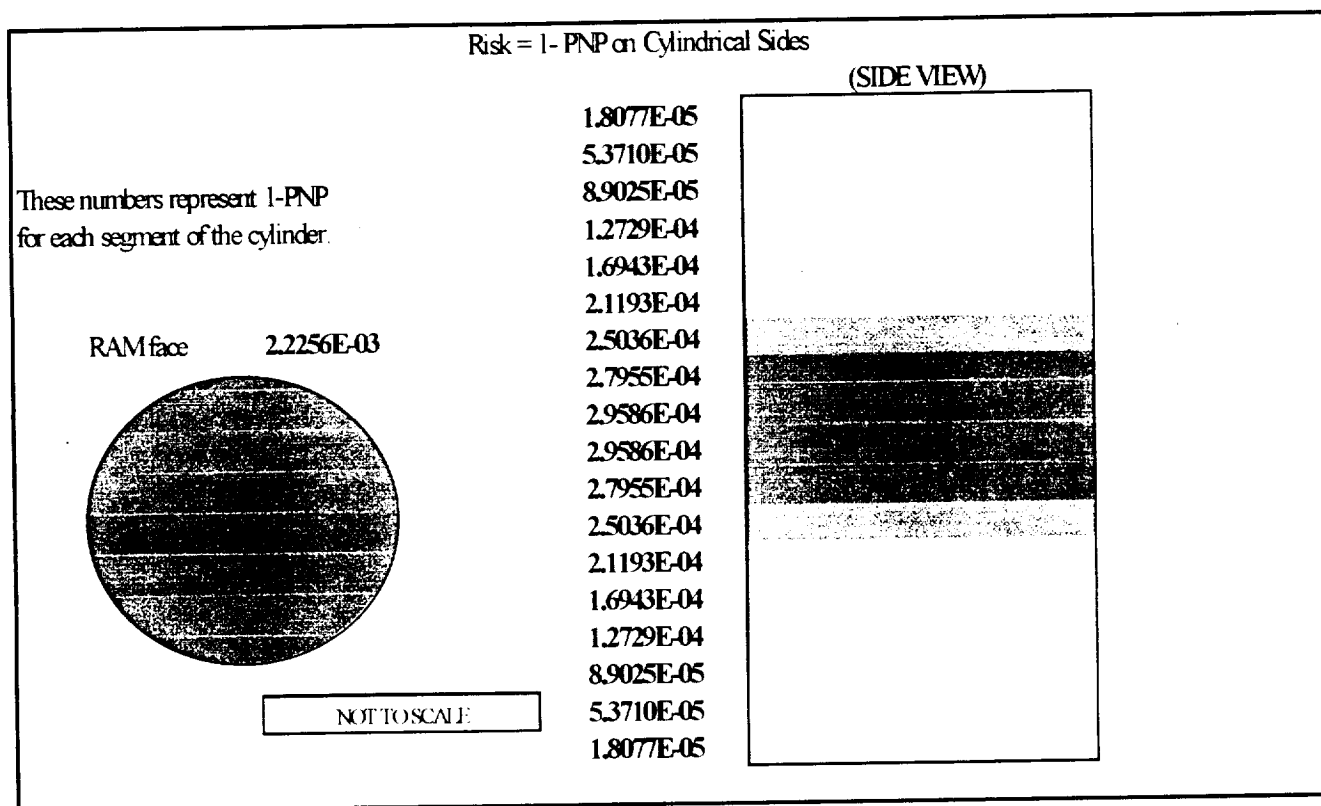


Figure 2.4.6-2. "Finite Segment" Results – Traditional Assessment (Stuffed Whipple Shield Configuration – Orbital Debris)

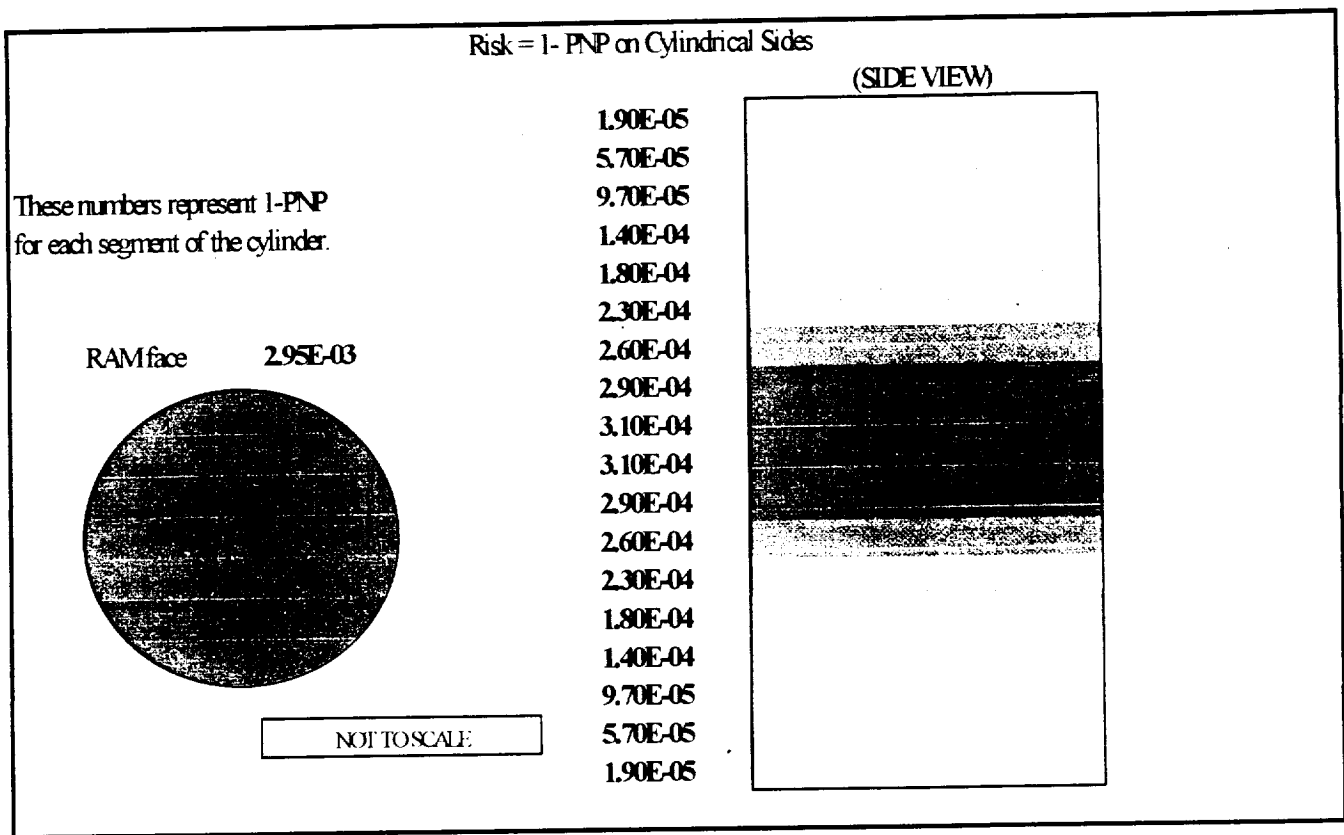


Figure 2.4.6-3. "Finite Segment" Results – Fractal Assessment (Stuffed Whipple Shield Configuration – Orbital Debris)

3.0 Conclusions

1. The meteoroid and orbital debris environment definitions pertinent to the ISS Propulsion Module fit fractal forms with a high degree of visual and statistical confidence.
2. The ORDEM96 orbital debris environment underestimates the flux relative to the NASA TM-4527 orbital debris environment definition for the ISS Propulsion Module.
3. Rectangular cross-sectional projected areas are self-similar and can be reduced and dealt with accordingly. While not strictly a fractal form, the self-similarity of these areas can be dealt with in a manner consistent with fractal forms.
4. Ballistic limit and crater phenomenology models pertinent to the ISS Propulsion Module fit fractal forms with a high degree of visual and statistical confidence.

5. Fractal risk assessments of ISS Propulsion Module orbital debris PNP for Whipple and Stuffed Whipple shielding configurations very closely estimate PNP values obtained by traditional spreadsheet analysis.
6. Fractal for Whipple Shield phenomenology model is excellent fit with correlation of 0.991 and significance level of 4×10^{-54} .
7. Fractal for "local" orbital debris flux model is excellent statistical and visual fit with correlation of 0.967 and significance level of 5.6×10^{-36} .
8. Non-fractal approximating model for Whipple Shield orbital debris velocity probability distribution is excellent statistical fit with correlation of 0.985 and significance level of 1.3×10^{-45} . Despite excellent statistical fit, non-fractal approximating model does not display good visual fit.
9. Revised preliminary standard (non-fractal) risk assessment indicates the probability of no orbital debris penetration (PNP) for ISS Propulsion Module Whipple Shield configuration is approximately 0.9876.
10. Preliminary fractal risk assessment for ISS Propulsion Module Whipple Shield configuration results in orbital debris PNP of 0.9891, a difference of 0.15% from the equivalent standard assessment.
11. Fractal for Stuffed Whipple Shield phenomenology model provides excellent statistical and visual fits with correlation of 0.9766 and significance level of 9.5×10^{-42} .
12. Fractal for "local" orbital debris flux model for Stuffed Whipple Shield is excellent statistical and visual fit with correlation of 0.9307 and significance level of 6.8×10^{-28} .
13. Revised preliminary standard (non-fractal) risk assessment indicates the probability of no orbital debris penetration (PNP) for ISS Propulsion Module Stuffed Whipple Shield configuration is approximately 0.9965.
14. Preliminary fractal risk assessment for ISS Propulsion Module Stuffed Whipple Shield configuration results in orbital debris PNP of 0.9955, a difference of 0.10% from the equivalent standard assessment.
15. Fractal crater phenomenology model shows excellent statistical fit with correlation of 0.922 and significance level of $3.03\text{E-}09$.
16. Fractal and traditional spreadsheet methodologies can result in meaningful "finite segment" risk assessments. Differences between the "finite segment" and "global" risk assessment PNP values are insignificant in both cases.

4.0 Recommendations

1. Use the TM-4527 environment model definitions with constant orbital debris particle density of 2.8 gm/cm^3 for Propulsion Module requirements and consistency with BUMPER.
2. Protect the ISS Propulsion Module to the same extent as the manned modules by using the Stuffed Whipple Shield design.
3. Perform fractal sensitivity analyses for other geometries, orbit parameters, and shield configurations.
4. Develop a generic fractal M/OD analysis spreadsheet.

5.0 References

Anderson, B.J., and Smith, R.E., "Natural Orbital Environment Guidelines for Use in Aerospace Vehicle Development," NASA TM-4527, June 1994.

Bunde, A., and Havlin, S., Fractals in Science, Springer-Verlag, 1994.

Christiansen, E.L., Crews, J.L., Williamsen, J.E., Robinson, J.H., and Nolen, A.M., "Enhanced Meteoroid and Orbital Debris Shielding," *International Journal of Impact Engineering*, Vol. 17, pp. 217-228, 1995.

Christiansen, E.L., "Design and Performance Equations for Advanced Meteoroid and Debris Shields," *International Journal of Impact Engineering*, Vol. 14, pp. 145-156, 1993.

Cour-Palais, B., "Meteoroid Environment Model – 1969 (Near-Earth to Lunar Surface)," NASA SP-8013, March 1969.

Crouch, E.A.C., and Wilson, R., Risk/Benefit Analysis, Ballinger Publishing Co., 1982.

Draper, N., and Smith, H., Applied Regression Analysis, John Wiley & Sons, 1981.

Drouin, M., Abou-Kandil, H., and Mariton, M., Control of Complex Systems: Methodology and Technology, Plenum Press, 1991.

Efron, B., "Bootstrap Methods: Another Look at the Jackknife," *The Annals of Statistics*, Vol. 7, No. 1, 1979.

Freudenberg, W.R., and Rursch, J.A., "The Risks of 'Putting the Numbers in Context': A Cautionary Tale," *Risk Analysis*, Vol. 14, No. 6, 1994.

Flood, R.L., and Carson, E.R., Dealing With Complexity: An Introduction to the Theory and Application of Systems Science, Plenum Press, 1988.

Ford, D.B., Personal Communication at MSFC, April 2001.

Hastings, H.M, and Sugihara, G., Fractals: A User's Guide for the Natural Sciences, Oxford University Press, 1995.

Harvard School of Public Health, "Analyzing Risk: Science, Assessment, and Management," September, 1994.

Juran, J.M., Juran's Quality Control Handbook, McGraw-Hill, Inc., 1988.

Klopp, R.W., Shockey, D.A., Osher, J.E., and Chau, H.H., "Characteristics of Hypervelocity Impact Debris Clouds," *International Journal of Impact Engineering*, Vol. 10, pp. 323-335, 1990.

Kronsjö, L., Computational Complexity of Sequential and Parallel Algorithms, John Wiley & Sons, 1985.

Lee, S.M.S., and Young, G.A., "Sequential Iterated Bootstrap Confidence Intervals," *Journal of the Royal Statistical Society*, Vol. 58, No. 1, 1996.

Lloyd, S., "Complexity Simplified," *Scientific American*, May 1996.

Mog, R.A., "Systems Engineering Metrics: Organizational Complexity and Product Quality Modeling," H-27289D, Final Report, OR Applications, September 1997.

Mog, R.A., "Risk Assessment Methodologies for Spacecraft in Particulate Environments: Enhancements Through Operations Research," OR Applications Final Report, September 1996.

Mog, R.A., "The Use of the Poisson Process in Environmental Risk Assessment," Internal Memo, July 1994.

Nemhauser, G.L., and Kan, A.H.G., Handbooks in Operations Research and Management Science: Computing, Vol. 3, North-Holland, 1992.

Nemhauser, G.L., Kan, A.H.G., and Todd, M.J., Handbooks in Operations Research and Management Science: Optimization, Vol. 1, North-Holland, 1989.

Neuts, M.F., Matrix-Geometric Solutions in Stochastic Models: An Algorithmic Approach, Dover Publications, Inc., 1981.

Nicolis, J.S., Chaos and Information Processing: A Heuristic Outline, World Scientific, 1991.

Papadimitriou, C.H., Computational Complexity, Addison-Wesley, 1994.

Peliti, L., and Vulpiani, A., Measures of Complexity, Springer-Verlag, 1988.

Sedgewick, R., Algorithms, Addison-Wesley, 1988.

Society for Risk Analysis, *Risk Analysis: Uncertainty Analysis*, Vol. 14, No. 4, August 1994.

Streufert, S., and Swezey, R.W., Complexity, Managers, and Organizations, Academic Press, Inc., 1986.

Thomas, D., and Mog, R., "A Quantitative Metric of System Development Complexity," 7th Annual INCOSE 1997 Symposium, August, 1997.

REPORT DOCUMENTATION PAGE			Form Approved OMB No. 0704-0188	
Public reporting burden for this collection of information is estimated to average 1 hour per response, including the time for reviewing instructions, searching existing data sources, gathering and maintaining the data needed, and completing and reviewing the collection of information. Send comments regarding this burden estimate or any other aspect of this collection of information, including suggestions for reducing this burden, to Washington Headquarters Services, Directorate for Information Operations and Reports, 1215 Jefferson Davis Highway, Suite 1204, Arlington, VA 22202-4302, and to the Office of Management and Budget, Paperwork Reduction Project (0704-0188), Washington, DC 20503.				
1. AGENCY USE ONLY (Leave blank)		2. REPORT DATE July 6, 2001		3. REPORT TYPE AND DATES COVERED Final Report
4. TITLE AND SUBTITLE Fractal Risk Assessment of ISS Propulsion Module in Meteoroid and Orbital Debris Environments			5. FUNDING NUMBERS H-33181D	
6. AUTHORS Robert A. Mog, Ph.D.				
7. PERFORMING ORGANIZATION NAME(S) AND ADDRESS(ES) OR Applications 7811 Lent Drive Huntsville, AL 35802			8. PERFORMING ORGANIZATION REPORT NUMBER	
9. SPONSORING/MONITORING AGENCY NAME(S) AND ADDRESS(ES) NASA-MSFC George C. Marshall Space Flight Center MSFC, AL 35812			10. SPONSORING/MONITORING AGENCY REPORT NUMBER	
11. SUPPLEMENTARY NOTES				
12a. DISTRIBUTION/AVAILABILITY STATEMENT Unlimited Distribution			12b. DISTRIBUTION CODE	
13. ABSTRACT (Maximum 200 words) <i>A unique and innovative risk assessment of the International Space Station (ISS) Propulsion Module is conducted using fractal modeling of the structural response to the meteoroid and orbital debris environments. Both the environment models and the structural failure modes due to resultant hypervelocity impact phenomenology, as well as Module geometry, are investigated for fractal applicability. The fractal risk assessment methodology produces a greatly simplified, but highly accurate alternative to current approaches, such as spreadsheet analyses and BUMPER code modeling, while maintaining or increasing the number of complex scenarios that can be assessed. As a minimum, this innovative fractal approach provides an independent assessment of existing methodologies in a unique way.</i>				
14. SUBJECT TERMS Complexity, Risk Assessment, International Space Station, meteoroids, orbital debris, fractals			15. NUMBER OF PAGES 65	
			16. PRICE CODE	
17. SECURITY CLASSIFICATION OF REPORT Unclassified	18. SECURITY CLASSIFICATION OF THIS PAGE Unclassified	19. SECURITY CLASSIFICATION OF ABSTRACT Unclassified	20. LIMITATION OF ABSTRACT UL	

NSN 7540-01-280-5500
FORM 298 (Rev 2-89)

Computer Generated

STANDARD

Prescribed by ANSI Std Z39-18

298-102